



Charged Cosmic Rays up to the knee region and beyond (II)

Antonella Castellina
Istituto Nazionale di Astrofisica
IFSI, Torino
e-mail: castellina@to.infn.it

Outline of the lecture

Introduction

Origin, acceleration and propagation

Models of the knee

Extensive Air Showers

Energy spectrum and composition

The measurement of the p-Air core

Anisotropy studies with EAS arrays

The Galactic to Extragalactic transition

Future projects

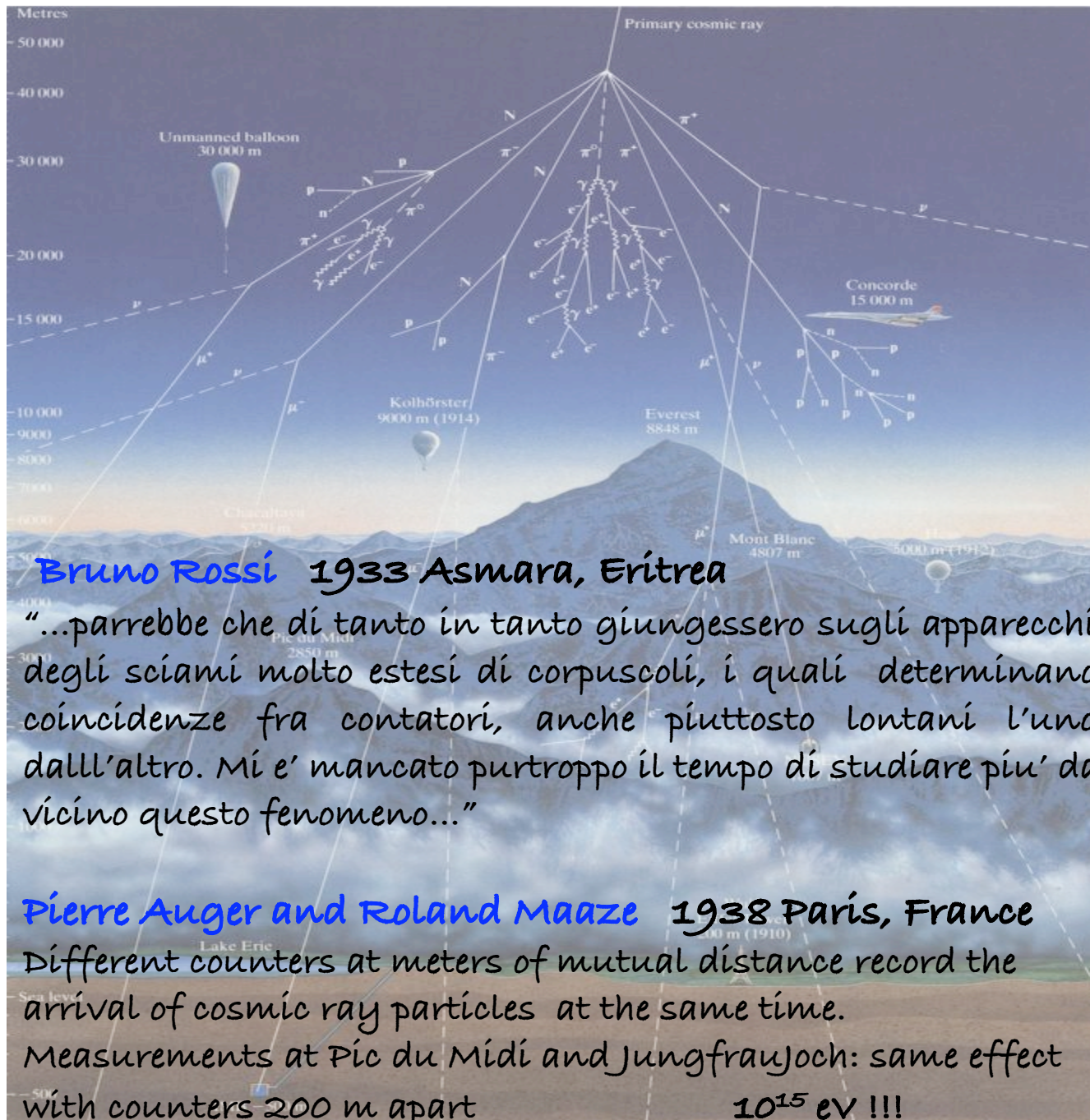
Discovery

The components of an EAS

Observables

Experimental techniques

Existing detectors



The discovery of the Extensive Air Showers

Bruno Rossi 1933 Asmara, Eritrea

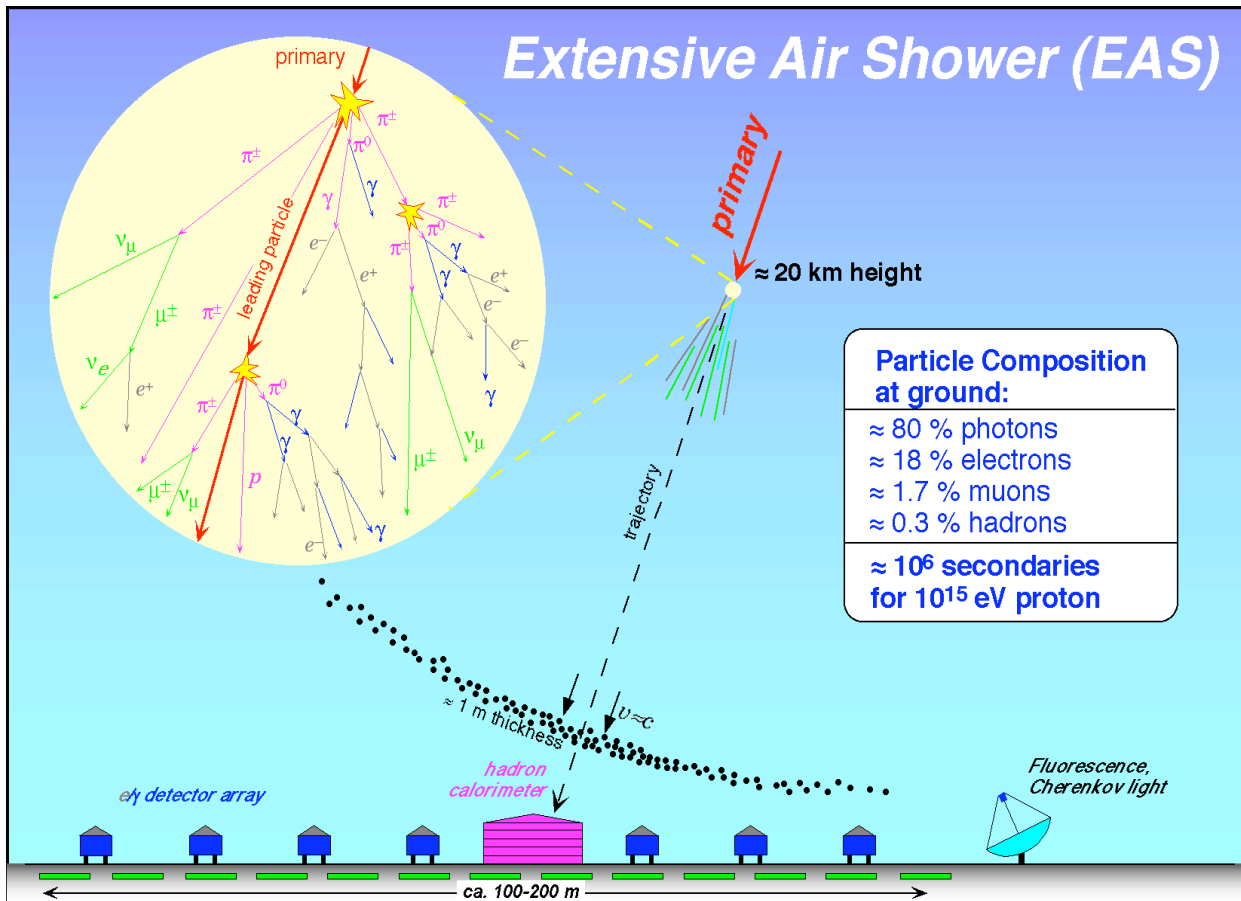
"...parrebbe che di tanto in tanto giungessero sugli apparecchi degli sciami molto estesi di corpuscoli, i quali determinano coincidenze fra contatori, anche piuttosto lontani l'uno dall'altro. Mi e' mancato purtroppo il tempo di studiare piu' da vicino questo fenomeno..."

Pierre Auger and Roland Maaze 1938 Paris, France

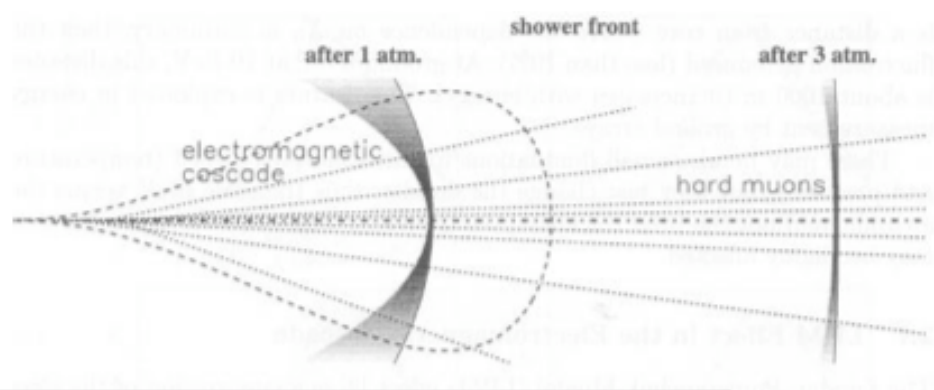
Different counters at meters of mutual distance record the arrival of cosmic ray particles at the same time.
 Measurements at Pic du Midi and Jungfrauoch: same effect with counters 200 m apart
 10^{15} eV !!!



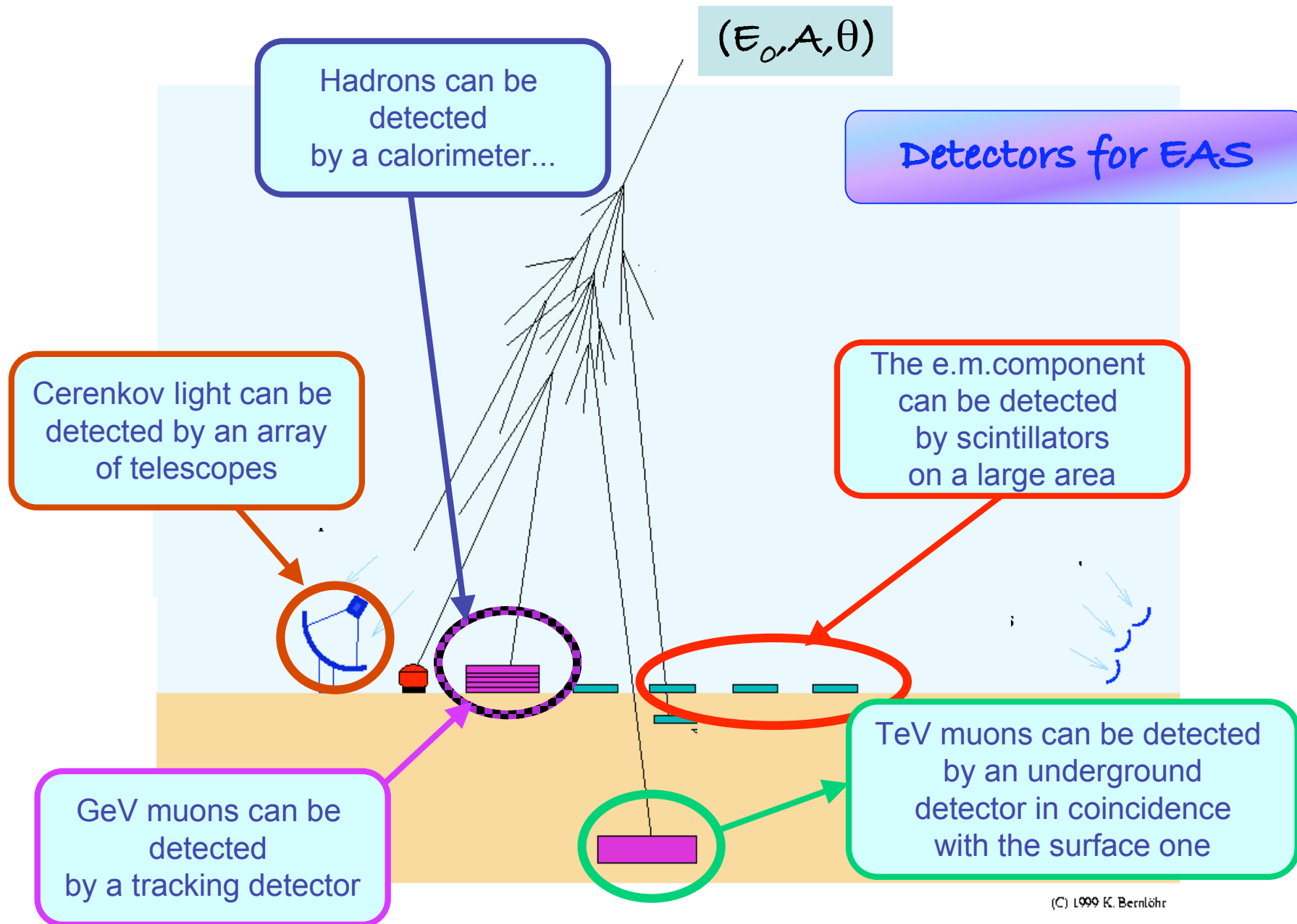
Extensive Air Shower (EAS)



Typical energies at ground:
 $\gamma, e \sim$ few MeV
 $\mu \sim$ few GeV



1 μ sec delay \rightarrow 300 m longitudinal distance



(C) 1999 K. Bernlöhr

Observables	Detectors
Number and fluctuation of electrons	scintillator arrays, water Cerenkov detectors
Number, energy, deflection angle, h_{prod} , fluctuation of μ	buried detectors, tracking calorimeters
Number, energy and distribution of hadrons	deep hadronic calorimeters
Number and distribution of Cerenkov photons	wide angle Cerenkov detectors
Cerenkov angular distribution	imaging Cerenkov telescopes
Depth of shower maximum	Cerenkov, fluorescence detectors

Observables in EAS

Charged particles:
 e^- , μ , hadrons
 Cerenkov light
 Fluorescence light

+

Monte Carlo simulations

E_0 , A
 hadronic interaction models
 + detectors response



Energy spectra
 Composition

Test of hadronic
 interaction
 models



Total area

E_{max}

Distance among counters

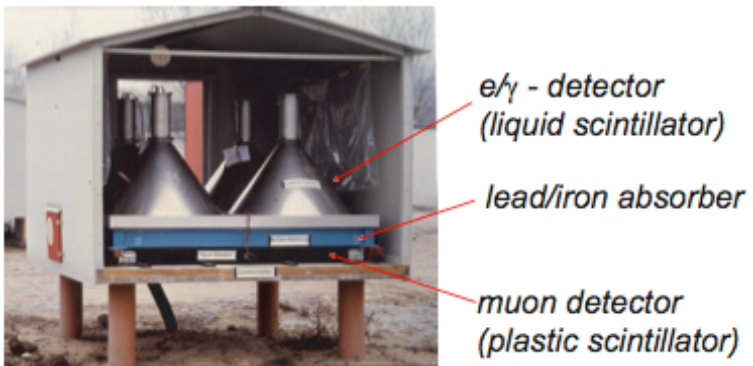
E_{min}

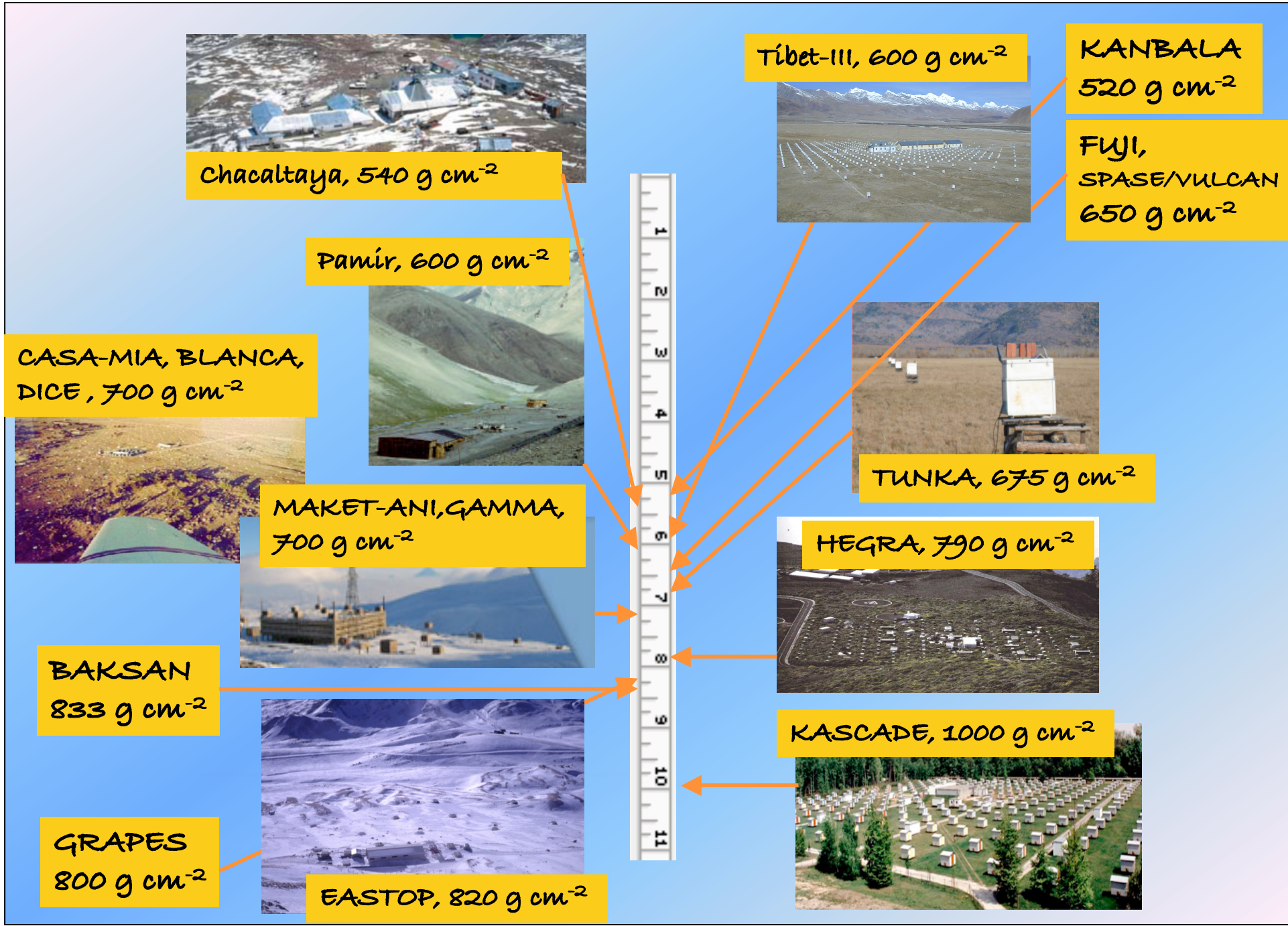
Number of counters

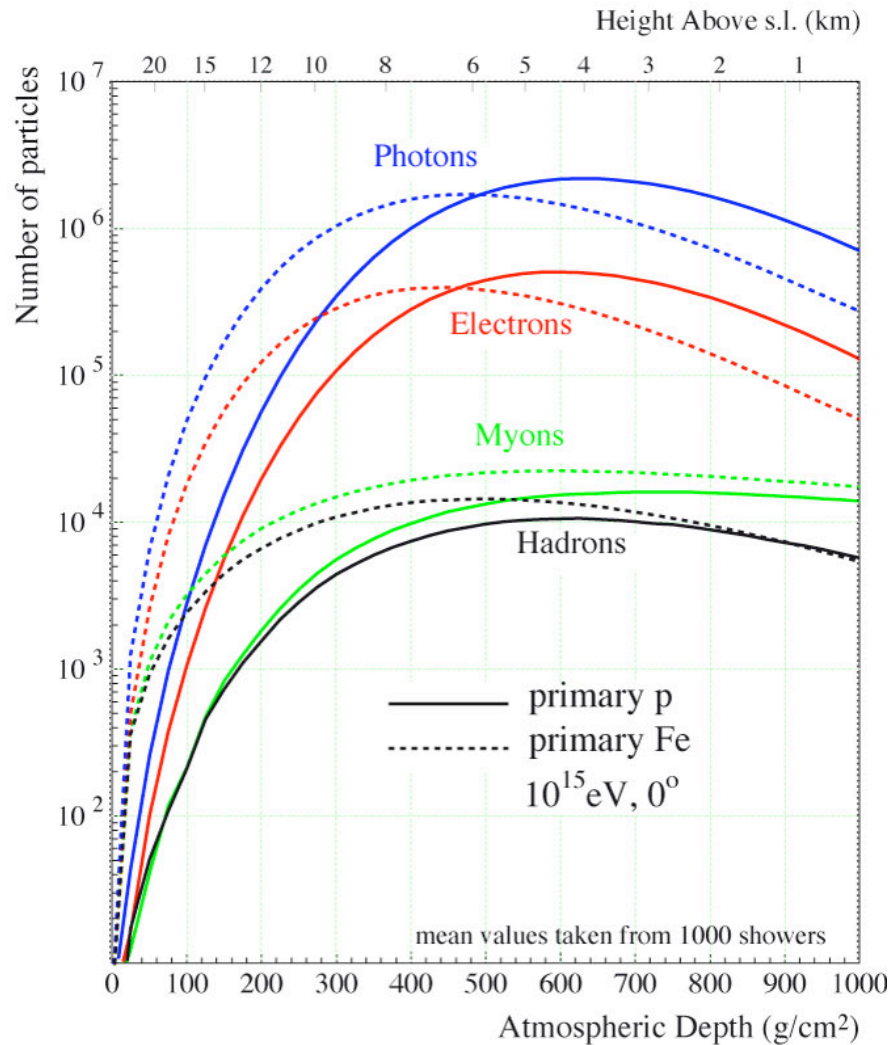
precision

Frequency in number of counting Φ_{part}

Arrival times in each counter θ_o



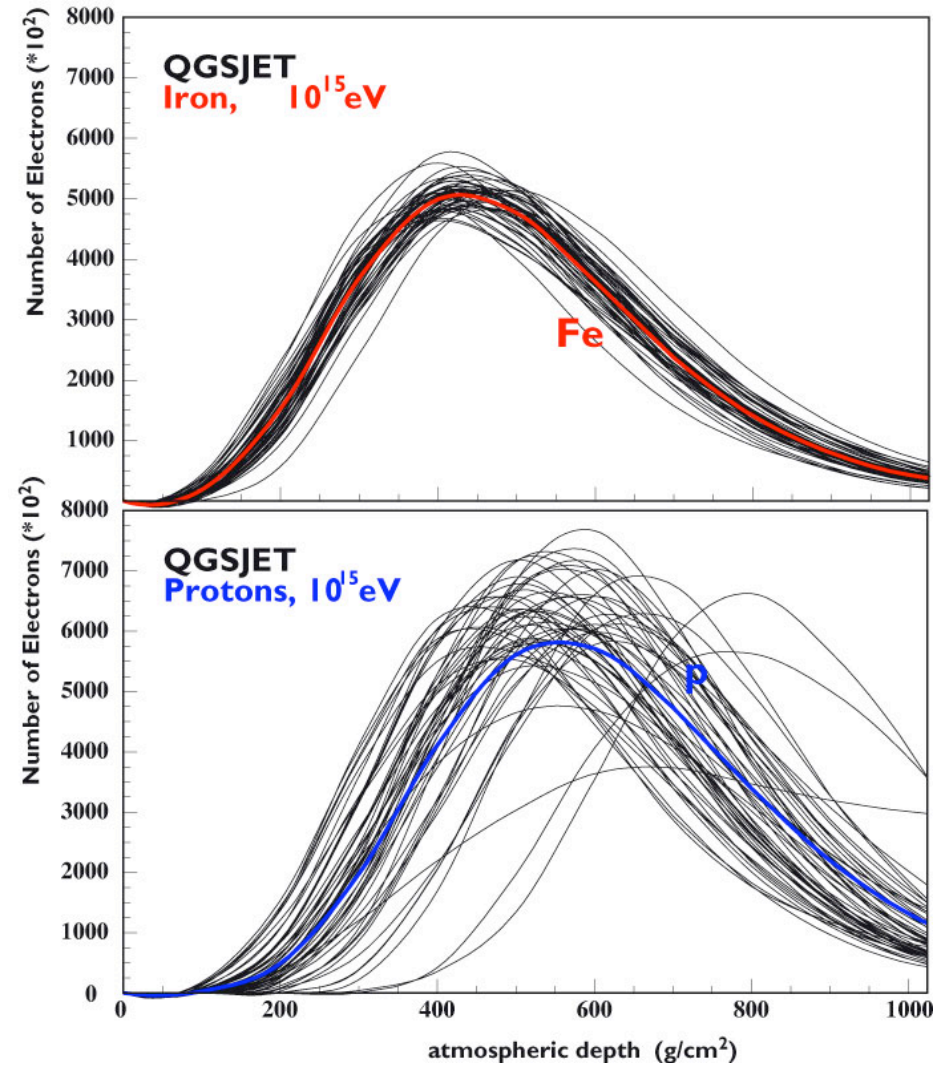




A primary Fe gives EAS with

- higher x_{max} [σ_{int} larger]
- more muons at ground
- less electrons at ground
- similar number of hadrons

The longitudinal development

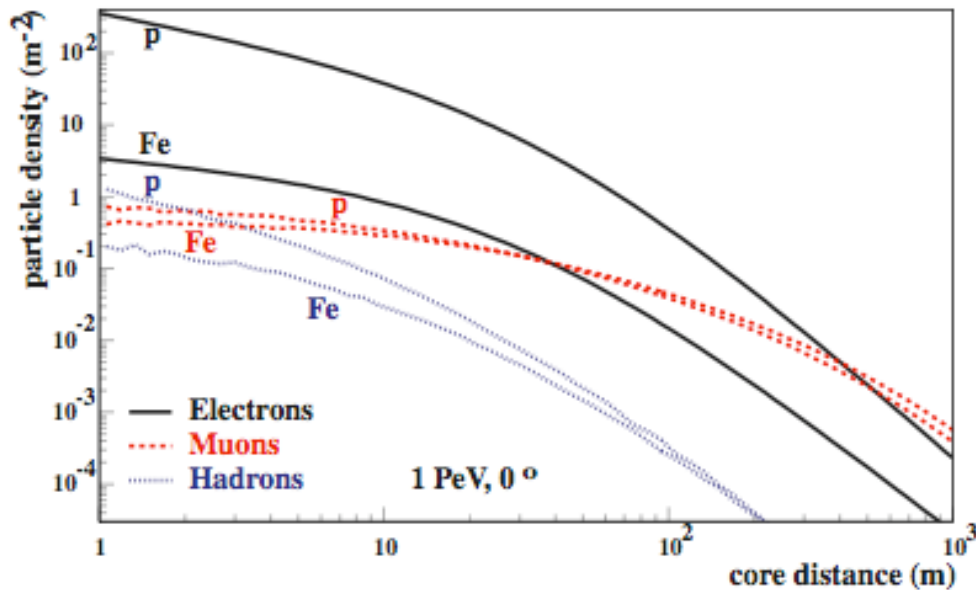
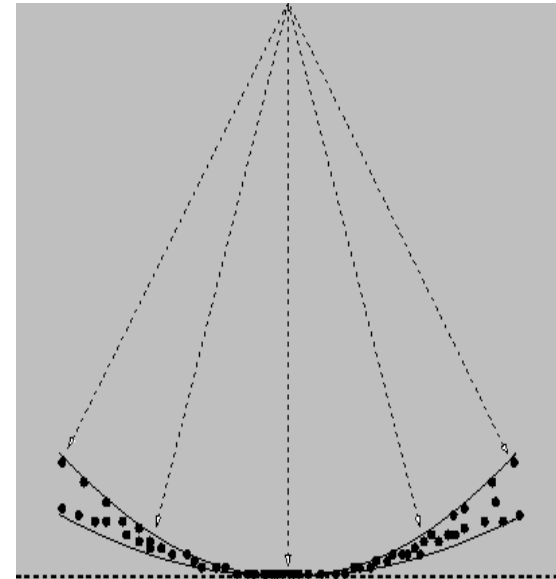


Fluctuations are lower for EAS from heavy nuclei

The em component

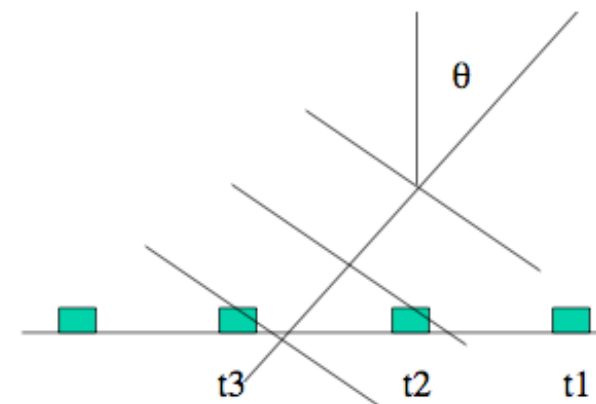
The shower size is determined through a fit of particle densities measured by different detectors to the NKG function

$$\rho_{ch} = \frac{N_{ch}}{2\pi r_0^2} \cdot C \cdot \left(\frac{r}{r_0}\right)^{s-2} \cdot \left(1 + \frac{r}{r_0}\right)^{s-4.5}$$

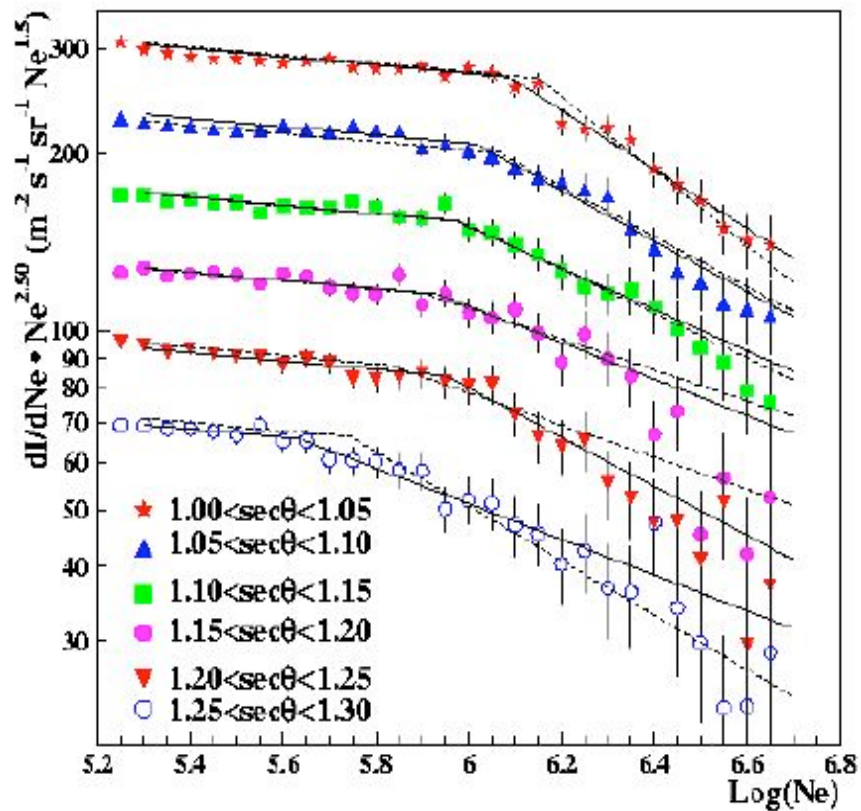


Scintillators / water detectors

The arrival direction is obtained from the relative times of arrival of the shower front at different detectors: $c\Delta t = d \cos\theta$



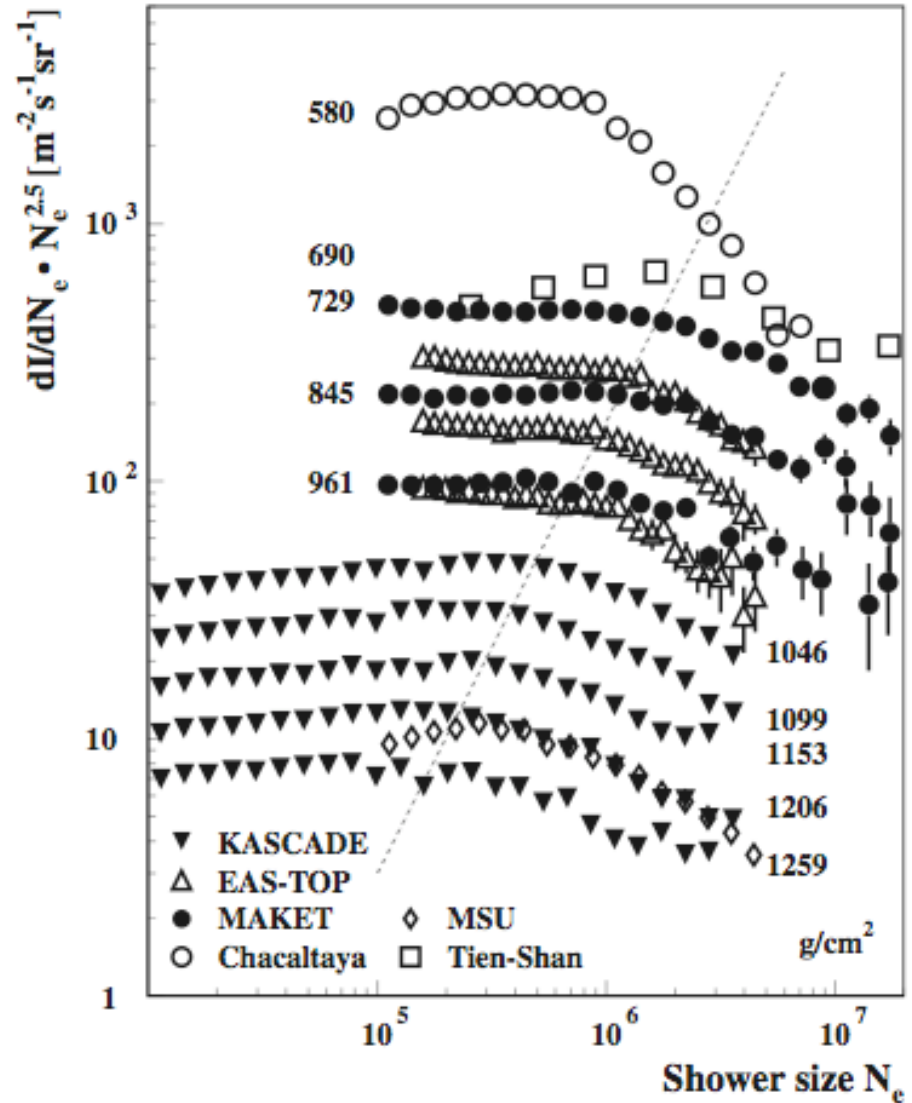
EASTOP



ELECTRON SIZE SPECTRUM:

- measure at different θ
- the size N_e^k at the knee energy decreases for increasing t
- $\Lambda_{EAS} = (219 \pm 3) \text{ g cm}^{-2}$

[M. Aglietta et al, *Astrop. Phys.* 10 (1999) 1]

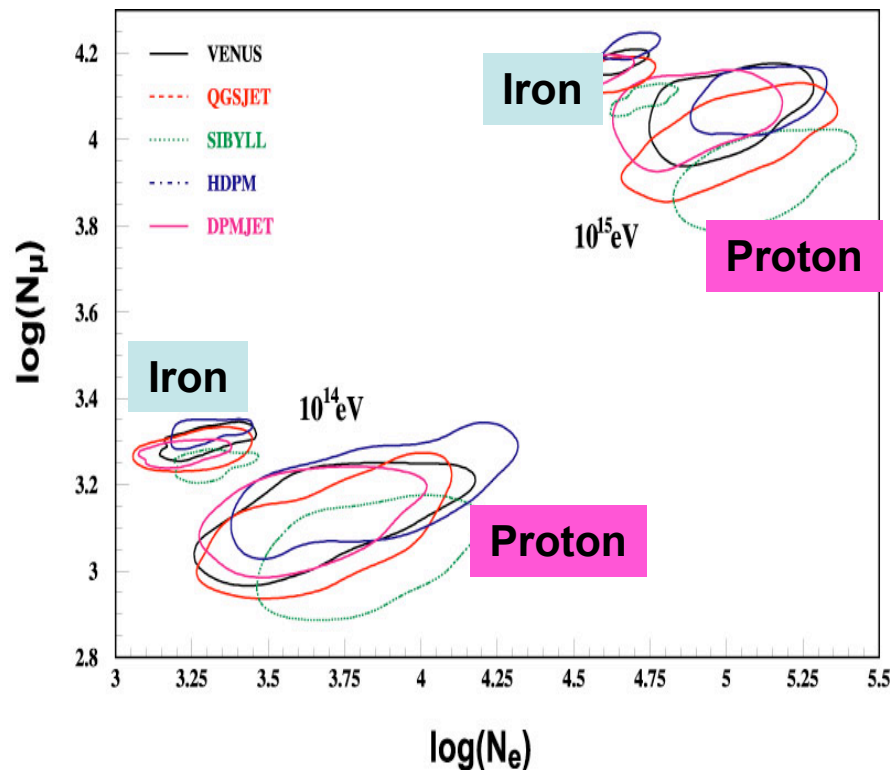


The μ component

The muon size comes from a fit to the muon densities measured at different distances from the shower core (LDF by Greisen in 1960)

$$\rho_{\mu}(r) \propto r^{-\alpha} \exp\left(-\frac{r}{r_0}\right)$$

$$N_{\mu}^{\text{tr}} = 2\pi \int_{r_0}^{r_1} \rho_{\mu}(r) r dr$$



μ component directly coupled to hadronic: link to properties of initial hadron

The number of low energy (GeV) and high energy (TeV) muons depends on primary atomic number

With N_e , the muon number is the most sensitive parameter to primary mass

Scintillators below absorber or tracking, water cerenkov tanks for GeV muons. Underground detectors for TeV muons

For a proton



$$N_{max} = E_0 / E_c$$

$$X_{max} = \lambda_1 \ln(E_0)$$

$$N_\mu = \left(\frac{E_0}{E_{dec}} \right)^\alpha$$

$$\alpha = \frac{\ln n_{ch}}{\ln n_{tot}} \approx 0.82 \dots 0.95$$

For heavier nuclei



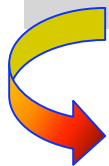
Superposition model:

A shower from a primary with mass A and energy E is equivalent to A showers of energy E/A

$$N_{max}^A = A E_n / E_c = E_0 / E_c$$

$$X_{max}^A \sim \lambda \ln(E_0 / A)$$

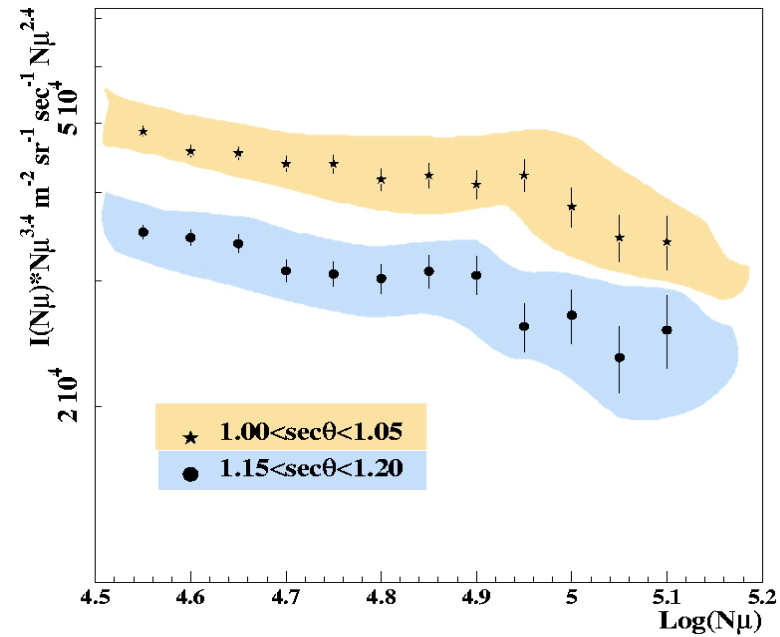
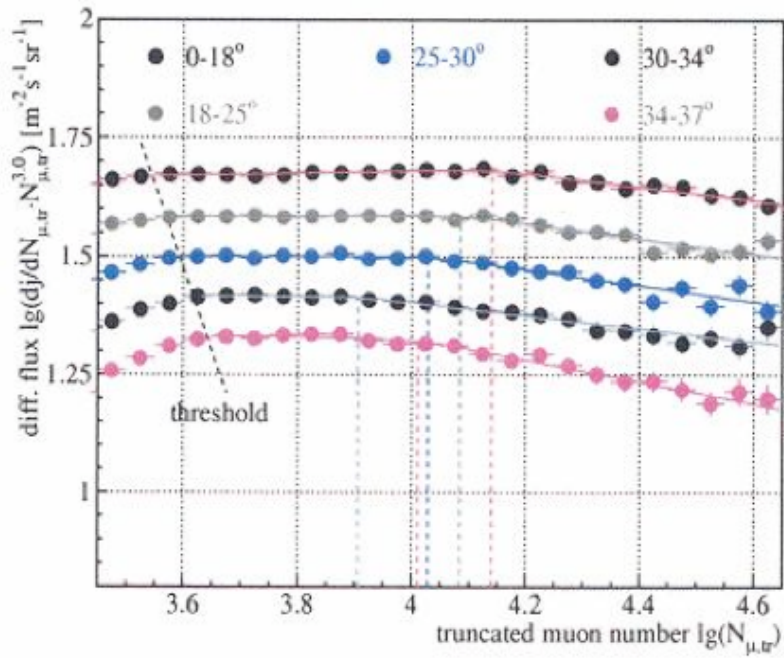
$$N_\mu^A = A \left(\frac{E_0 / A}{E_{dec}} \right)^\alpha = A^{1-\alpha} N_\mu$$



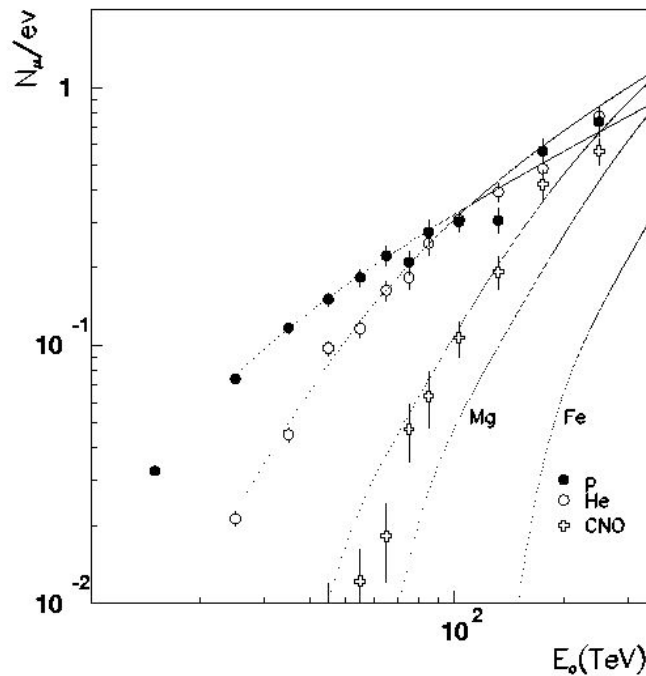
$$D_e = dX_{max} / d \ln E \sim \lambda (1 - d \ln A / d \ln E)$$

elongation rate

$$(D_{10} = 2.3 D_e)$$



GeV μ



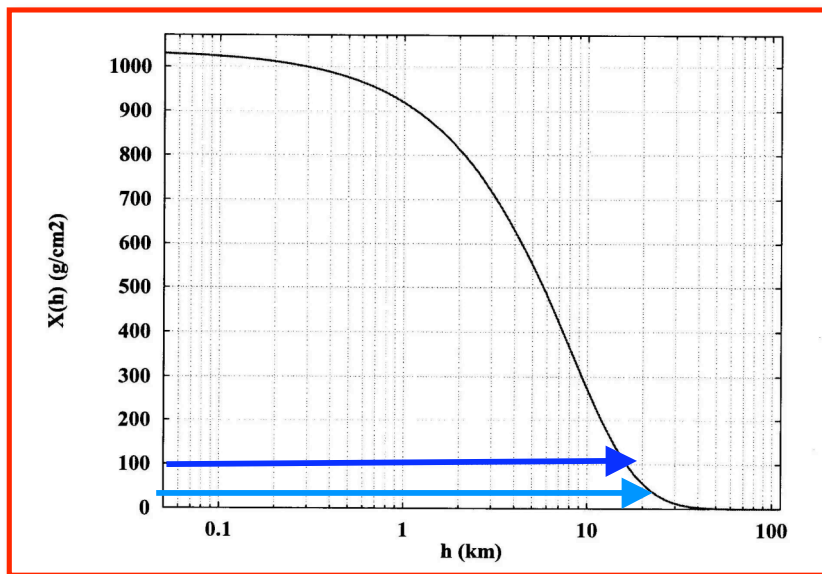
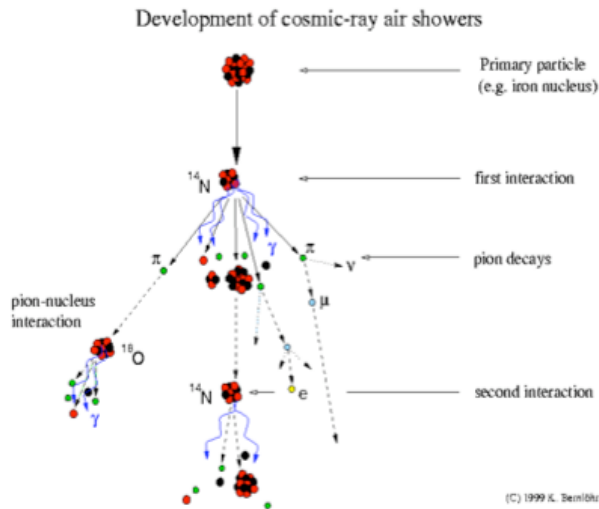
GeV μ from Cascade and Eas-Top



TeV μ from underground detectors

MACRO - EASTOP
BAKSAN - BUST
SPASE - AMANDA

...



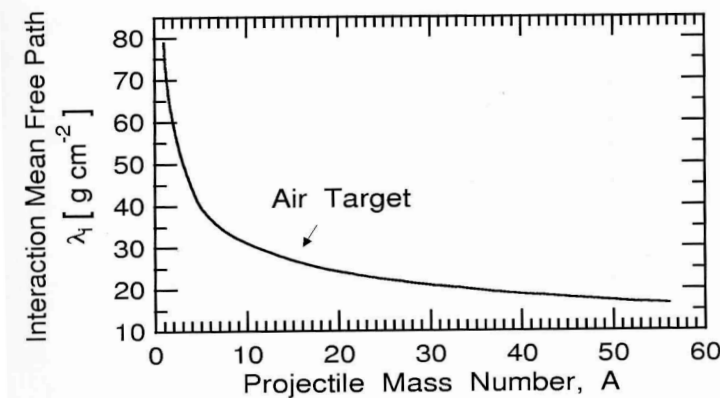
Burst detectors (high altitude),
hadron calorimeters.

The hadronic component

Back bone of the air shower (hadronic core). They constantly feed the em component of the EAS through π^0 s.

Secondary hadrons produced in early stages of showers

Reminder of first interaction features. Total number of hadrons nearly proportional to primary energy



The Cerenkov light

$n_{\text{air}} = 1.00029$ (at sea level)
 $E_{\text{ch}}(e) = 21 \text{ MeV}$ (35 MeV
at 7.5 km)



Almost all electrons
of the EAS emit
Cherenkov light.

Maximum opening angle
of emitted light $\approx 1.3^\circ$
(at sea level)



All C-light associated to EAS
contained in a narrow cone,
keeping the shower direction

Weak absorption of light
in atmosphere



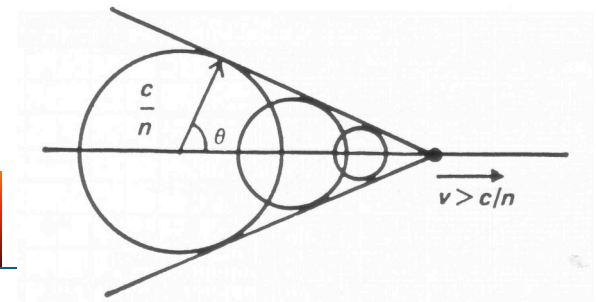
Most C-light reaches observation
level. $N_{\text{ph}} \propto L_{\text{tr}}$ above observer, a
very good measure of E_0 .

Lateral distribution and
temporal structure depend on
shower max position



Information on longitudinal
development. Primary mass

C-light detectors = reflectors + PMTs.



Outline of the lecture

Introduction

Origin, acceleration and propagation of cosmic rays

Models of the knee

Extensive Air Showers

Energy spectrum and composition
measurements and results

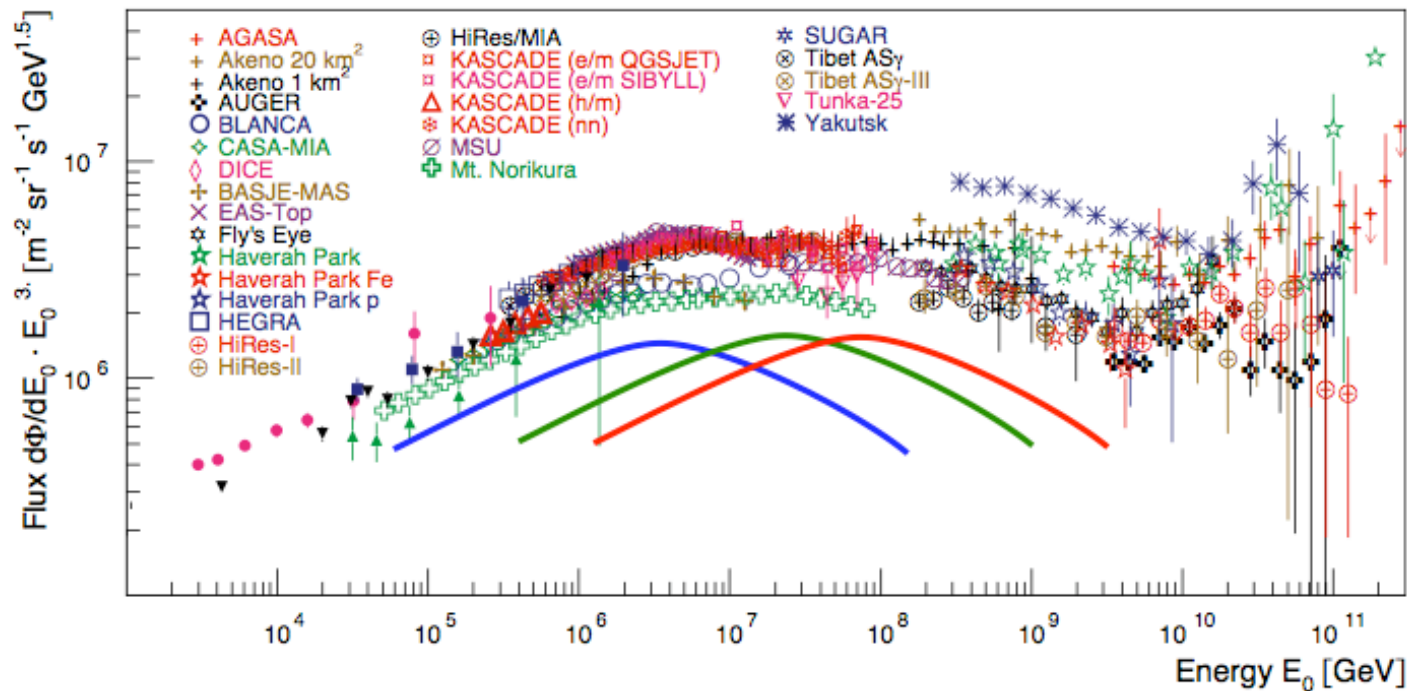
The measurement of the p-Air cross section

Anisotropy studies with EAS arrays

The Galactic to Extragalactic transition

Future projects

The all-particle energy spectrum
The link with direct measurement:
spectra and comp. below the knee
The high energy region
Cerenkov detector results
Models of the knee: comparison
with data



Energy and composition are strictly related information

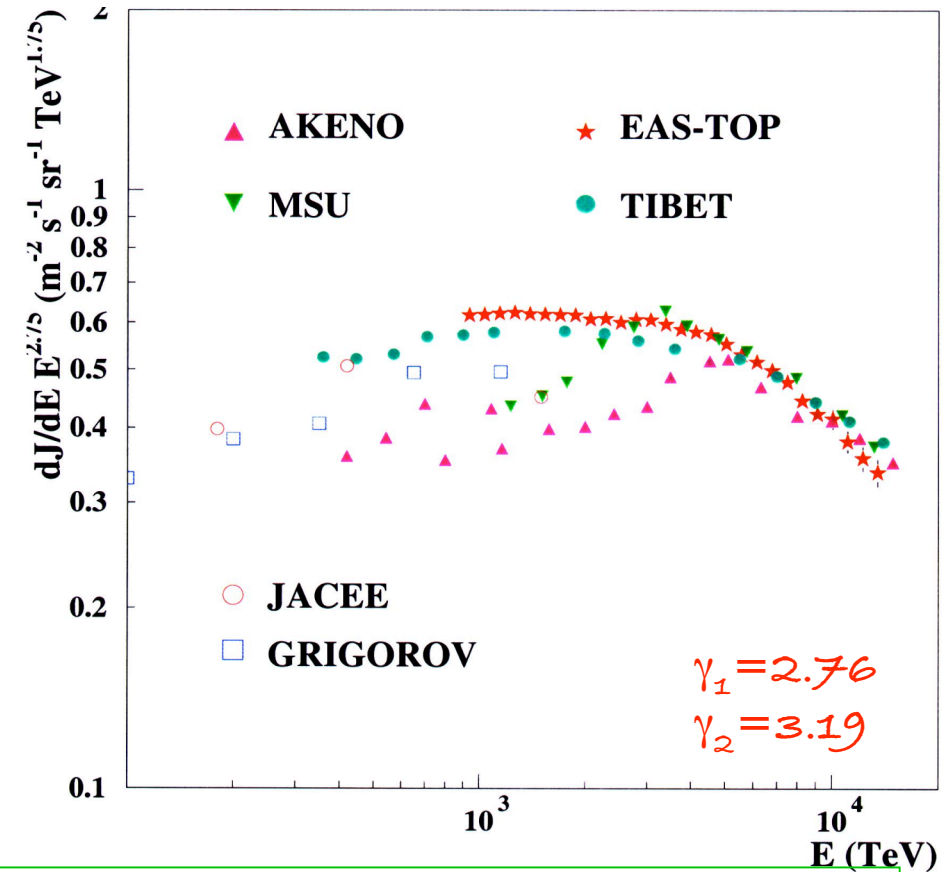
All observables are derived either from the lateral spread of EAS at a specific observation level or from its longitudinal development in atmosphere

Multi-detector arrays are more powerful, since they can correlate different observables

The understanding of data relies on the knowledge of the stochastic and systematic uncertainties.

The conversion from the observable to the physical quantity relies on Monte Carlo simulations

EAS-TOP



N_e converted to 810 g cm^{-2} using the measured $\Lambda_{\text{abs}} = (219 \pm 3) \text{ g cm}^{-2}$

Corsika code + interaction model

$$N_e(E_o, A) = \alpha(A) E_o^{\beta(A)}$$

Effective A from direct measurements, with

$$E_k(A) = Z \times E_k^p(A)$$

Extrapolation checked by consistence with other measurements

Systematic uncertainties from model and composition, each 10 %.

[M. Aglietta et al., *Astrop. Phys.* 10 (1999) 1]

CASA-MIA

1089 particle detectors (0.25 km²)

1024 muon detectors, 3 m underground

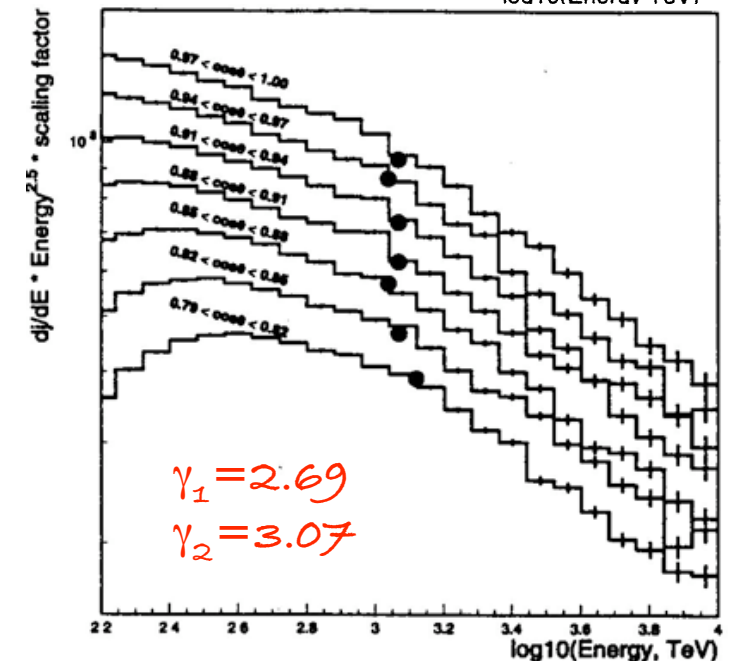
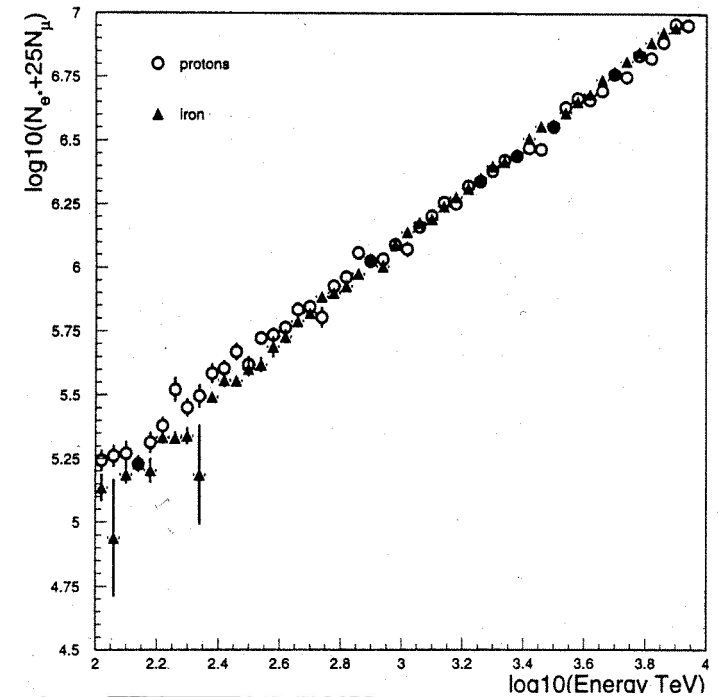
$$F = \log(N_e + \xi N_\mu) \quad \rightarrow$$

- F does not depend on A: systematic differences in energy assignment less than 5%
- F depends very little on θ but remains independent on composition
- ξ dependent on the model

the energy is determined independently from composition

the knee does not change with θ

[M. Glasmacher et al., *Astrop. Phys.* 10 (1999) 291]



KASCADE



200 × 200 m² at 1020 g/cm²

Array: 252 detector stations with e/γ- and muon counters

Central detector: 300 m² hadron calorimeter and 4 muon layers

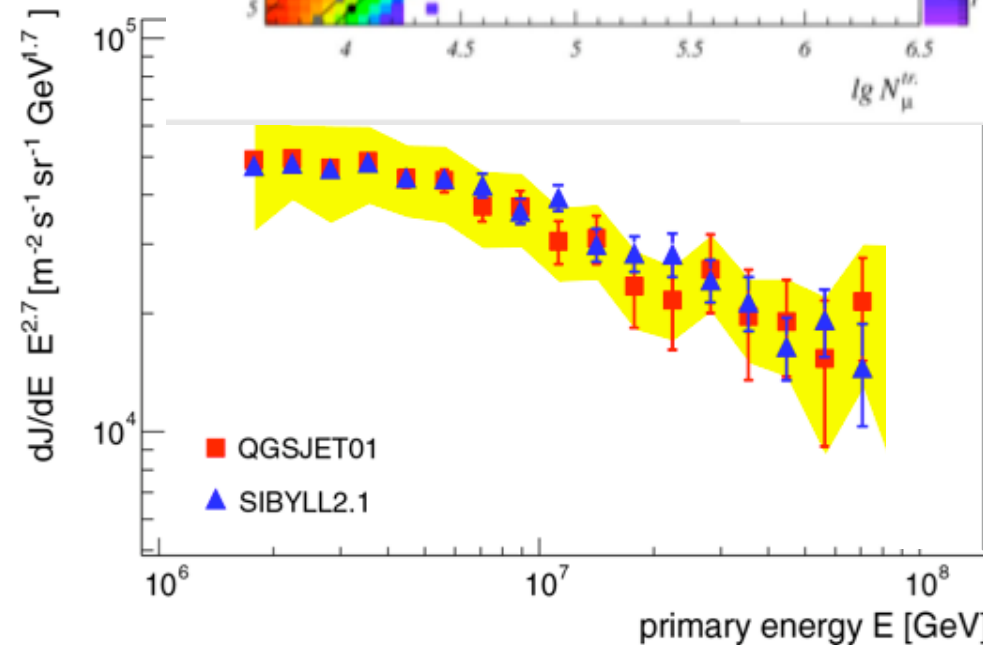
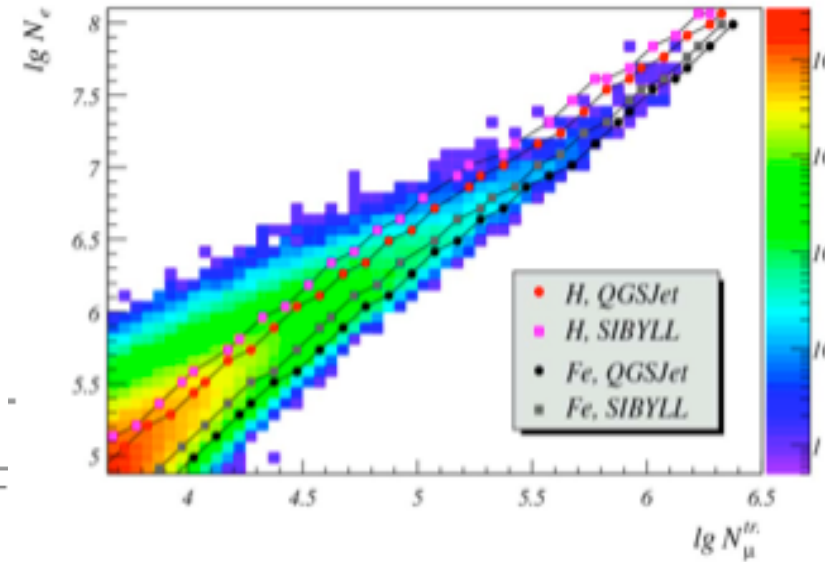
MTD: 120 m² muon tunnel

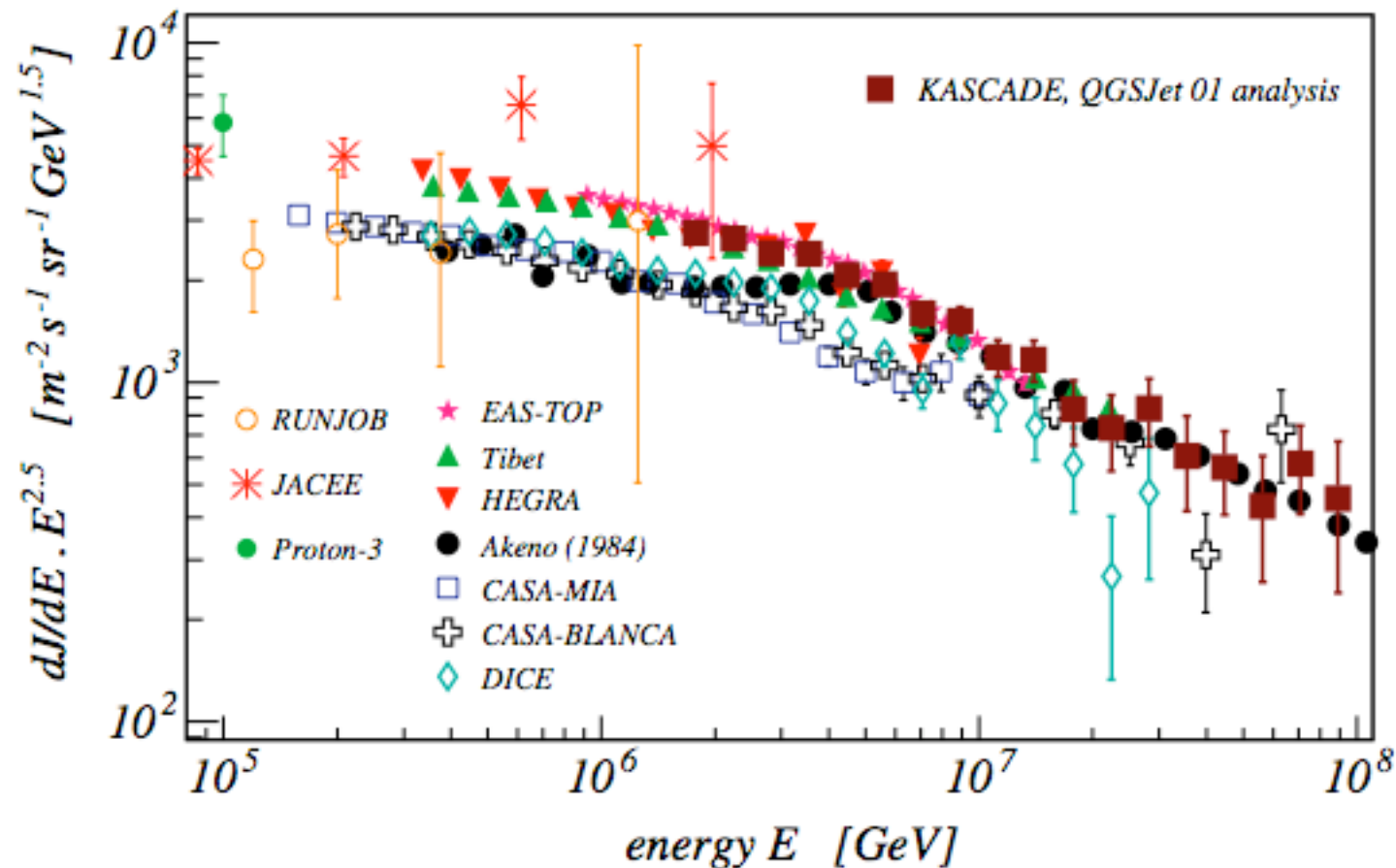
Combined χ^2 minimization to fit N_e, N_μ size spectra simultaneously

$$\frac{dJ}{d\log N_e d\log N_\mu} = \sum_A \int_{-\infty}^{+\infty} \frac{dJ_A}{d\log E} p_A(\log N_e, \log N_\mu | \log E) d\log E$$

The all particle spectrum : sum of 5 mass groups spectra

[T. Antoni et al., *Astrop. Phys.* 24 (2005) 1]





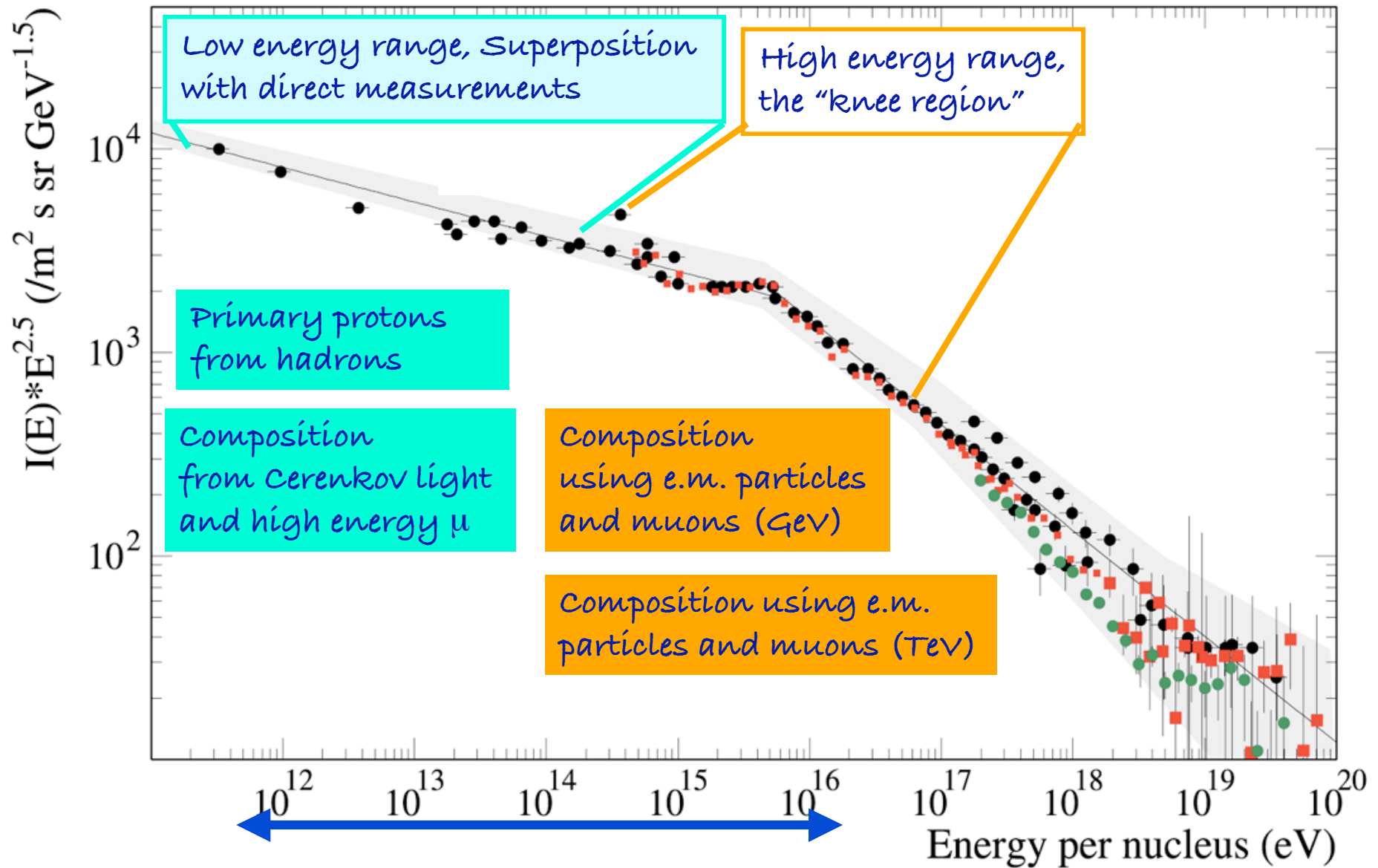
The spectra agree quite well in shape and knee position (despite different techniques, observables, atmospheric depths!)

15% systematic shift in energy needed to match fluxes

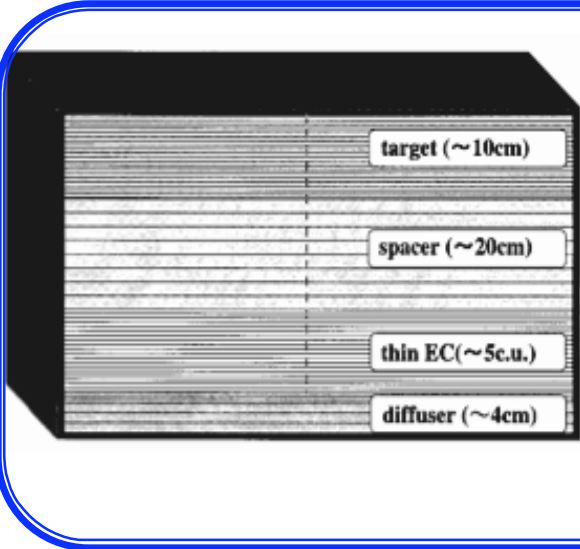
Smooth knee at ~ 4 PeV, $\gamma_{\text{below}} \sim 2.7$, $\gamma_{\text{above}} \sim 3.1$

...but need different mass groups spectra to discriminate among astrophysical models!

Spectrum and composition information



Direct measurements with balloons

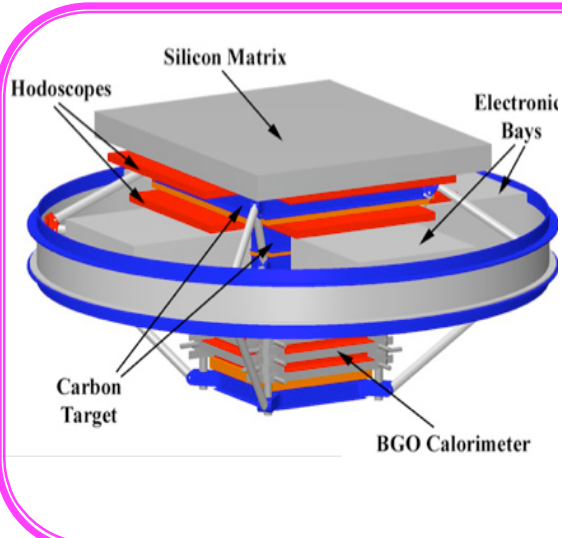
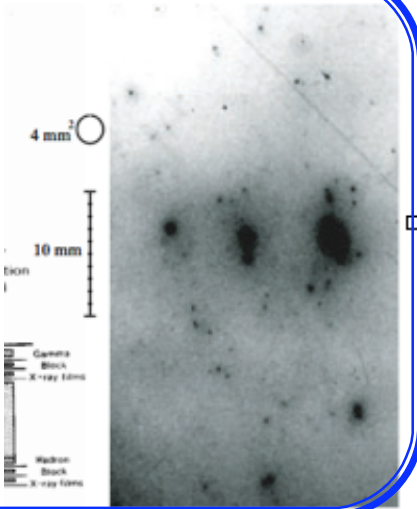


RUNJOB, JACEE

Passive detectors with nuclear emulsions

- must be recovered and developed in laboratory
- record the incoming particle and secondaries from interaction

p, He, heavy nuclei up to 500 TeV/nucleon



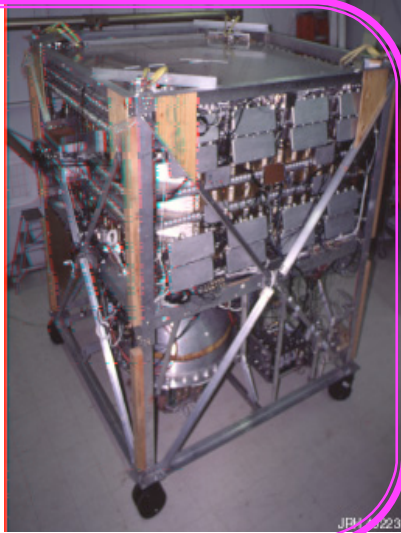
ATIC, TRACER, CREAM

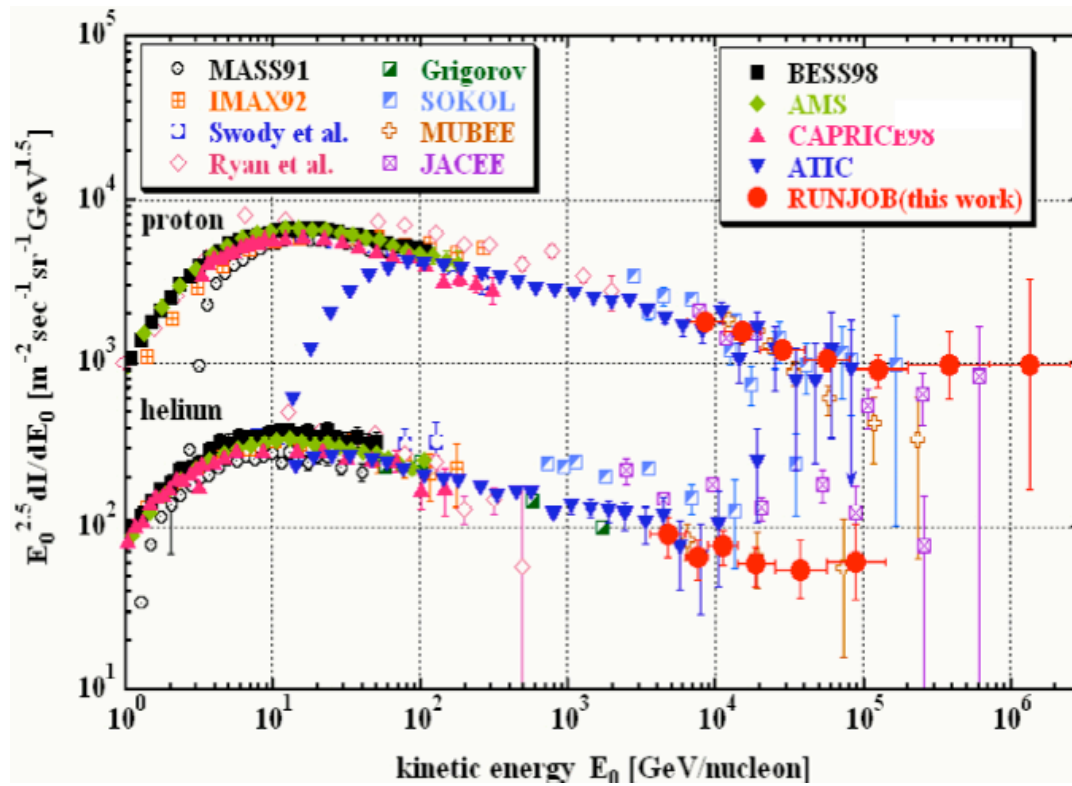
Include detectors for charge measurement (fine grain silicon matrix, scintillators) and for energy evaluation (calorimeters, transition radiation detectors,)

p-Ni from 50 GeV to 100 TeV total energy

O-Fe from 1 GeV/n to 10 TeV/n

p-Fe from 10^{11} to 10^{15} eV

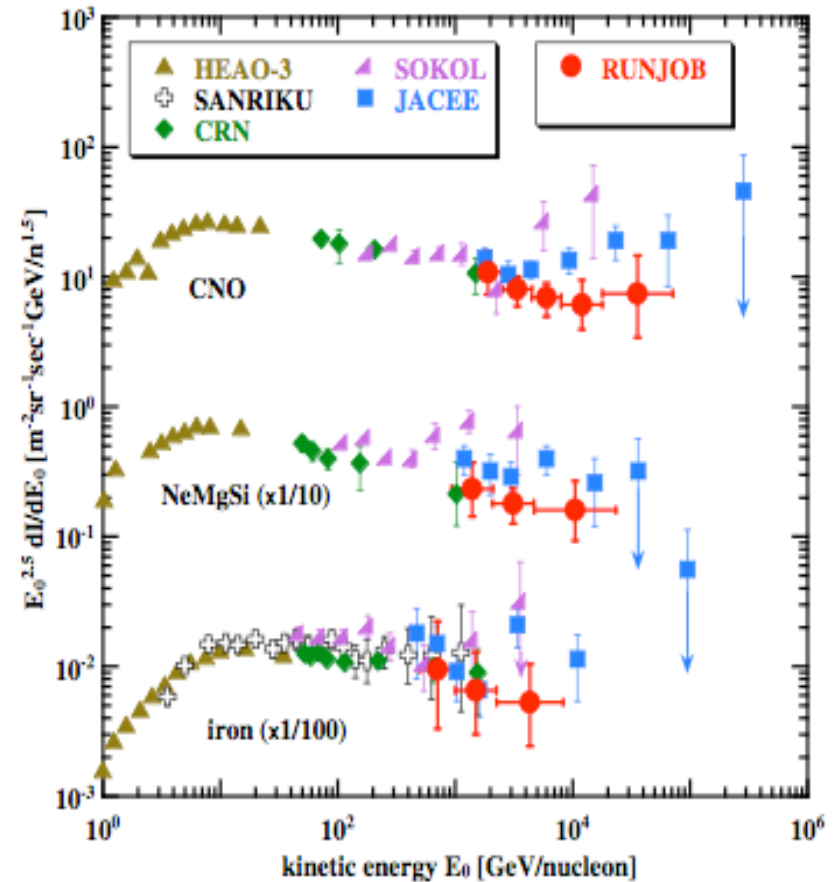




RUNJOB $\gamma_p \approx 2.74 \pm 0.08$
 $\gamma_{He} \approx 2.78 \pm 0.20$
 JACEE $\gamma_p \approx 2.80, \gamma_{He} \approx 2.68$

 He(RUNJOB) $\sim 1/2$ He(JACEE)
 at $E = 100$ TeV/n

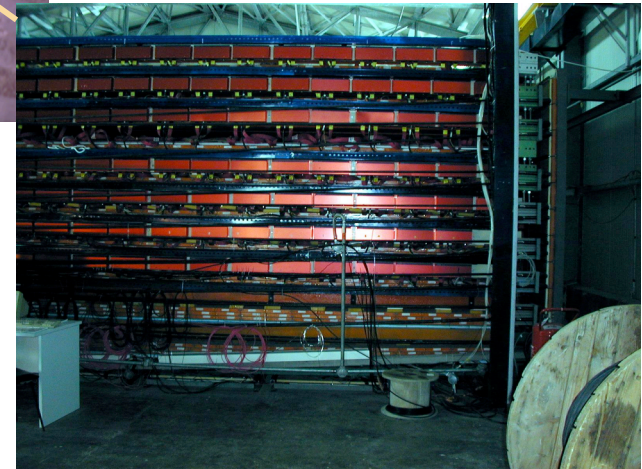
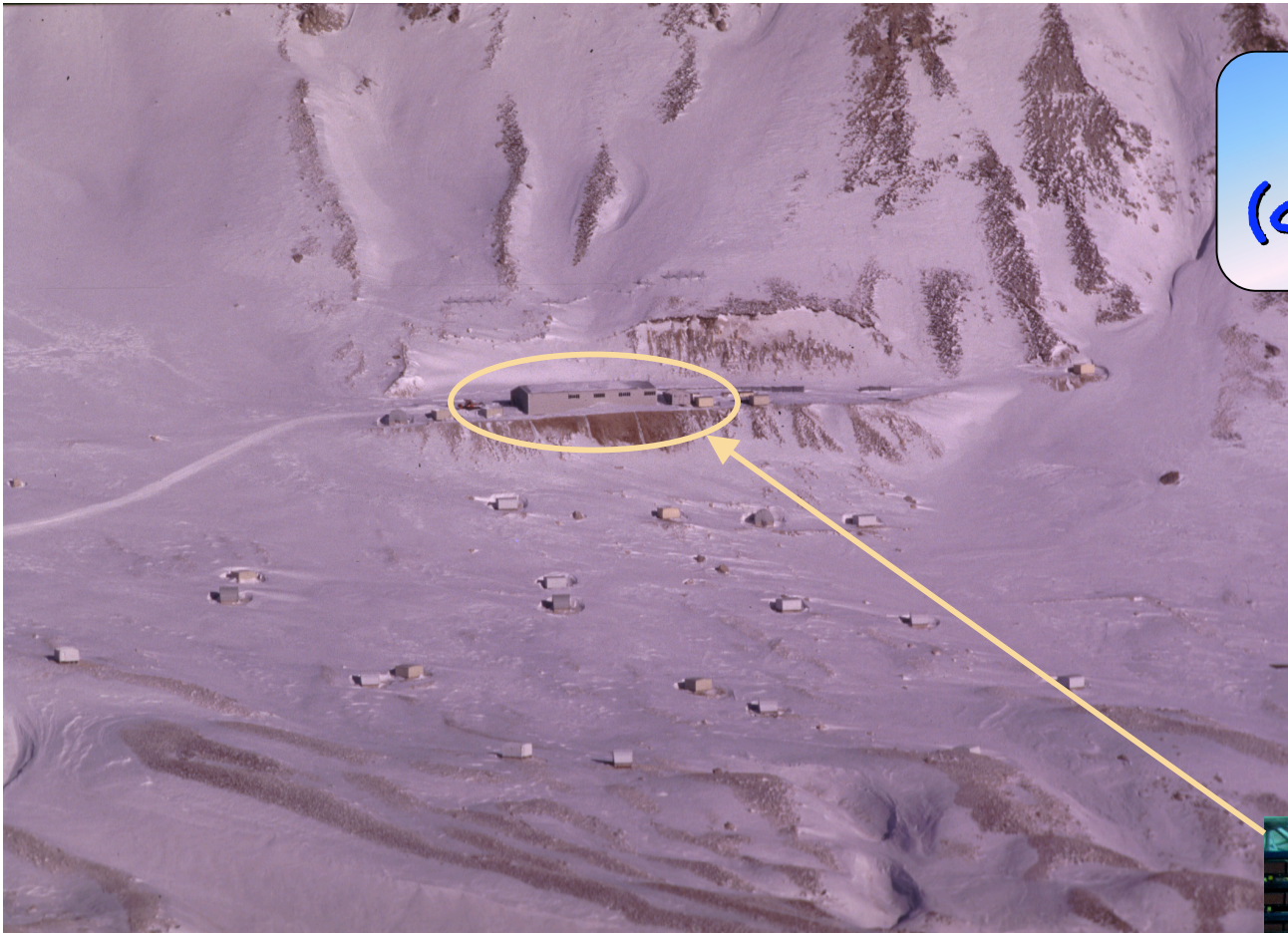
RUNJOB: $\gamma \sim 2.7$ for CNO to ~ 2.6 for Fe
 If Runjob/Sanriku gradual change in
 slope indicated a rigidity
 dependent form
 If JACEE/Sokol different sources for
 protons and for He and heavier



[V.A.Derbina et al, Astrop.J 628 (2005)]

EAS-TOP (Gran Sasso, Italy)

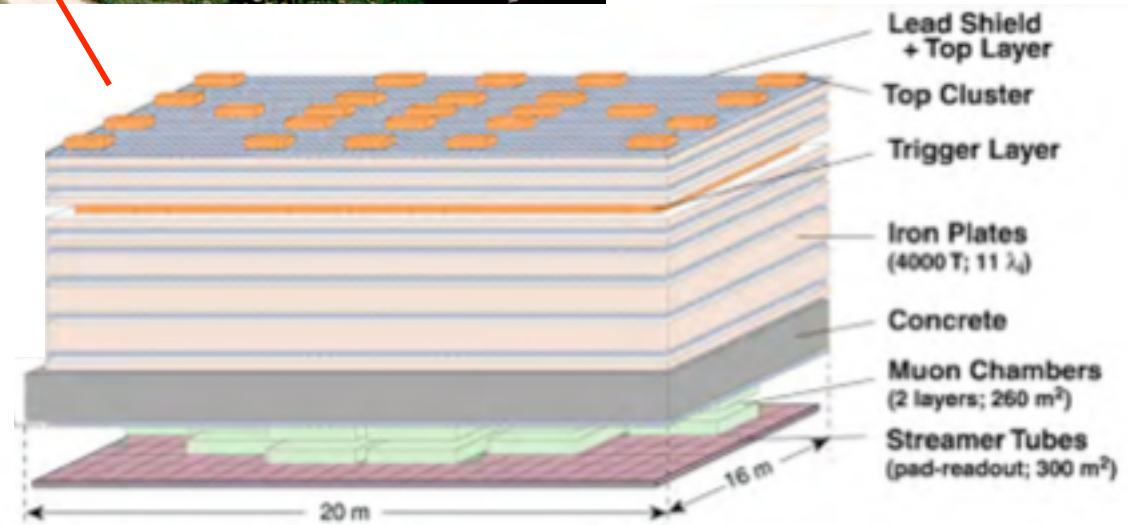
2000 m asl
820 g cm⁻²



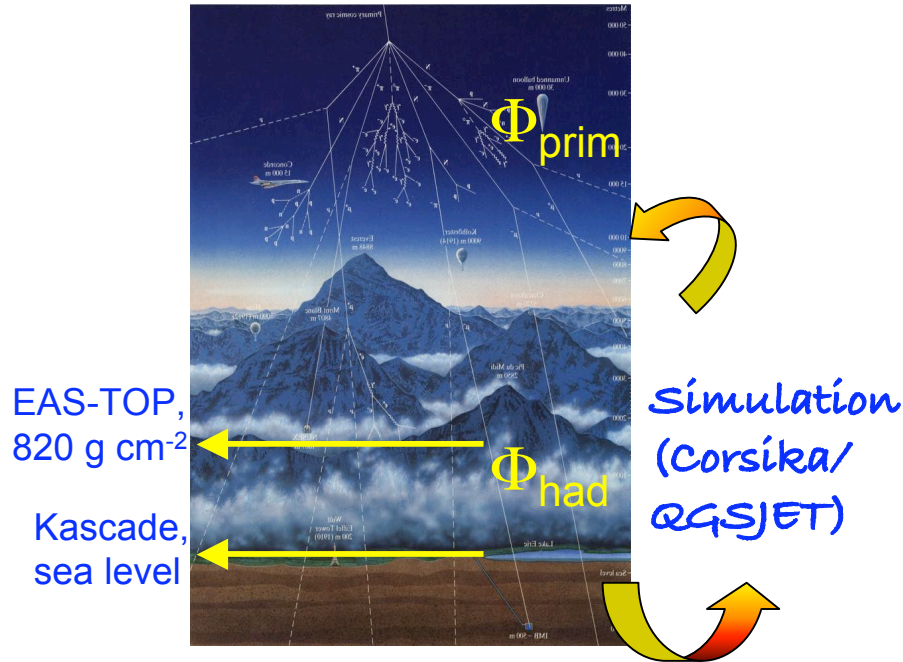
144 m² Hadron calorimeter:
9 layers x 13 cm Fe absorber,
2 layers streamer tubes
1 layer "quasi-proportional" tubes

KASCADE (Karlsruhe, D)

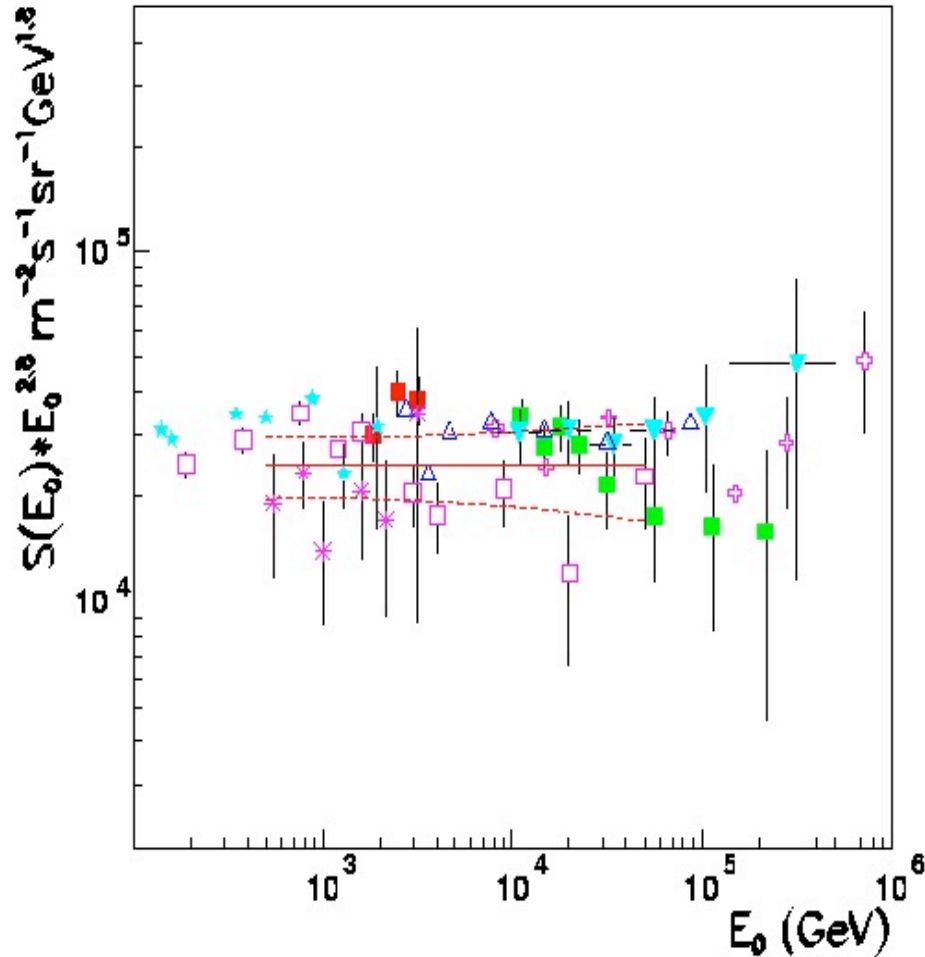
110 m asl
1100 g cm⁻²



Proton primaries
from hadron data



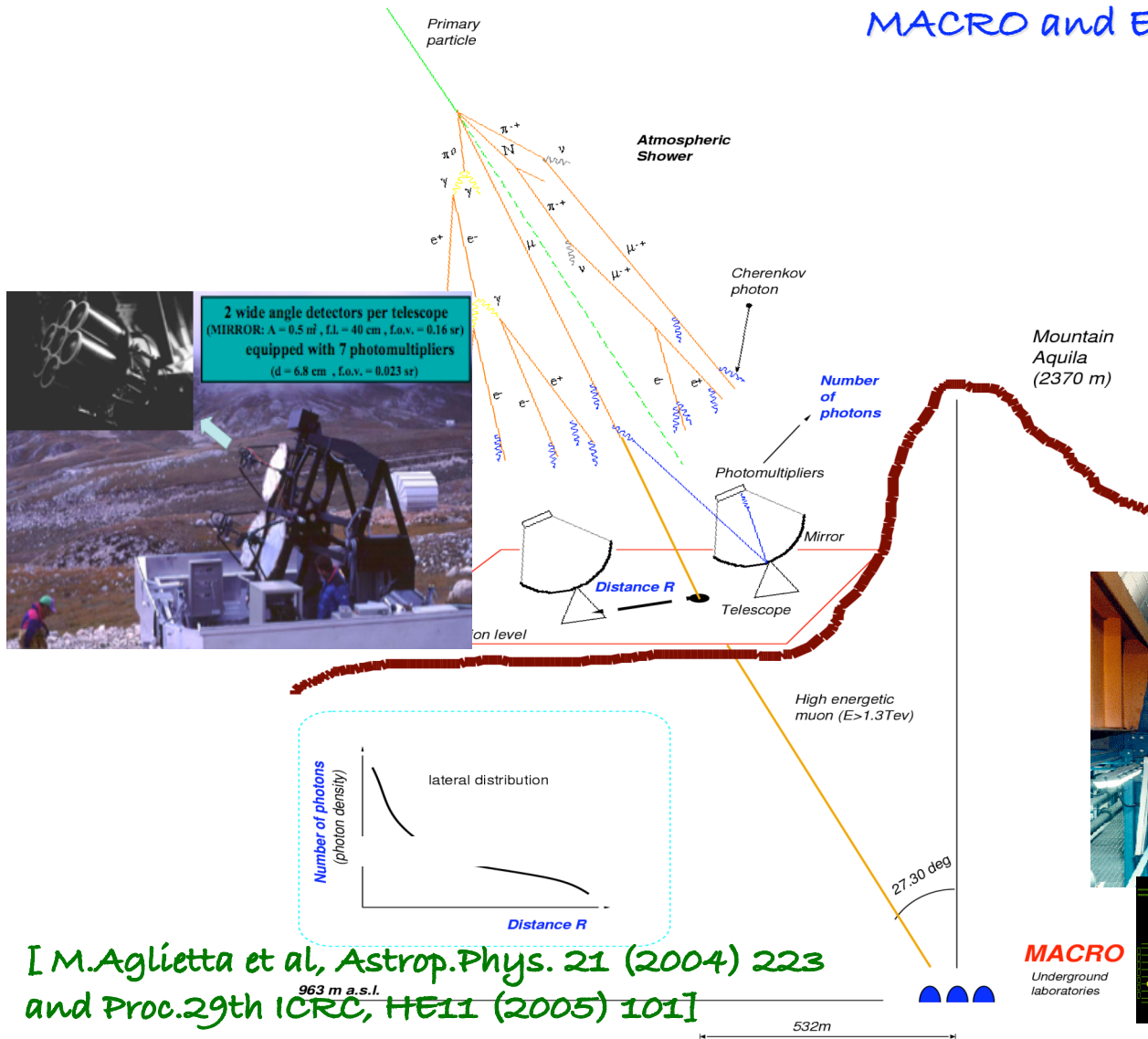
Measure the flux of single hadrons
 use Monte Carlo to subtract the Helium contribution to the hadron flux
 CORSIKA/QGSJET tested in EAS data:
 the model reproduces the experimental ratio at better than 10%
 Minimize the difference between measured and expected (from different proton spectra)
 hadron flux



[M.Aglietta et al, Astrop.Phys. 19 (2003) 329
 T.Antoni et al., ApJ 612 (2004) 914]

Composition from Cerenkov light and HE muons

MACRO and EAS-TOP separated by 1100 - 1300 m of rock
 ($E_{\mu} \gg 1.3 - 1.8 \text{ TeV}$)
 Common angular field
 $16^{\circ} < \theta < 58^{\circ}, 127^{\circ} < \phi < 210^{\circ}$



$76.6 \times 12 \times 4.8 \text{ m}^3$
 $E_{\mu} \sim 1.3 \text{ TeV}$

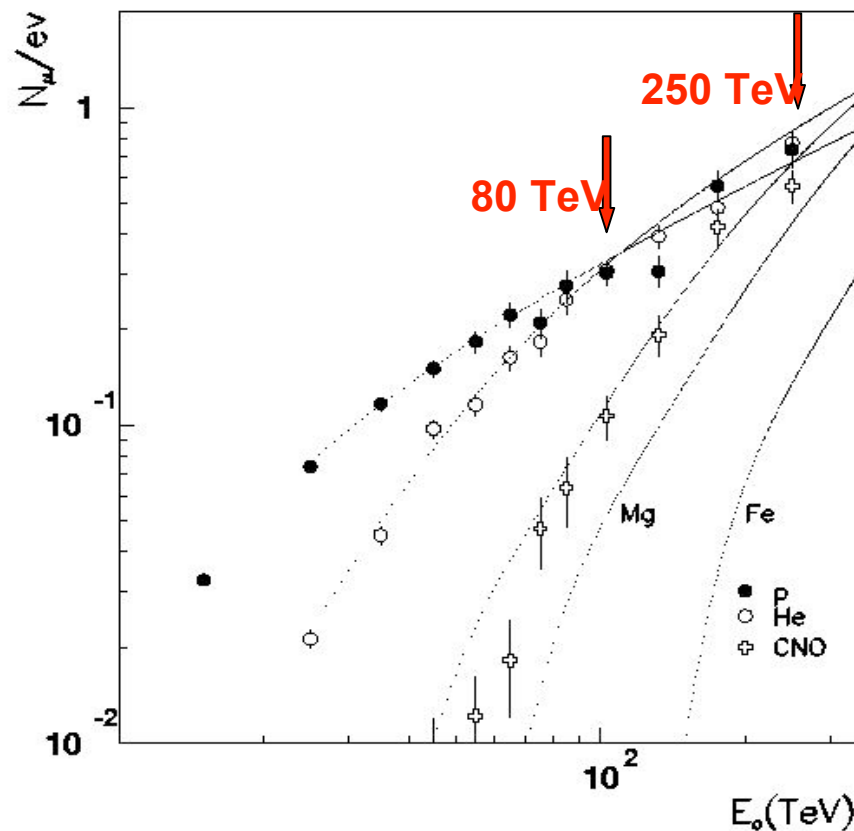


[M. Aglietta et al, *Astrop. Phys.* 21 (2004) 223
 and Proc. 29th ICRC, HE11 (2005) 101]

What is measured:

MACRO : selection of primaries based on the energy/nucleon by means of the TeV μ and EAS geometry by means of the muon tracking ($E_{\mu}^{\text{thr}} \sim 1.3 \text{ TeV}$)

EASTOP : Cerenkov light intensity and average Cerenkov lateral distribution ($E^{\text{thr}} = 20 \text{ TeV}$)



Key points of the analysis:

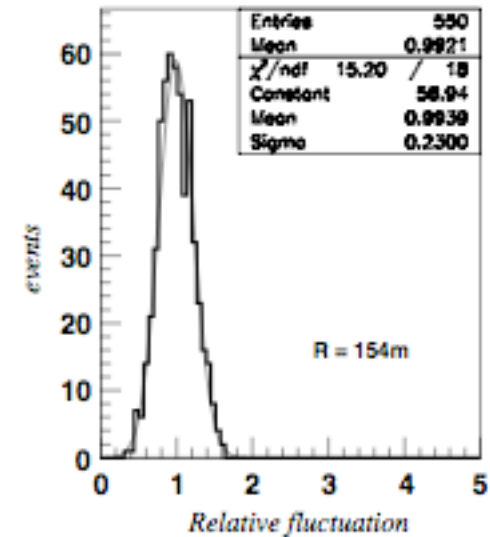
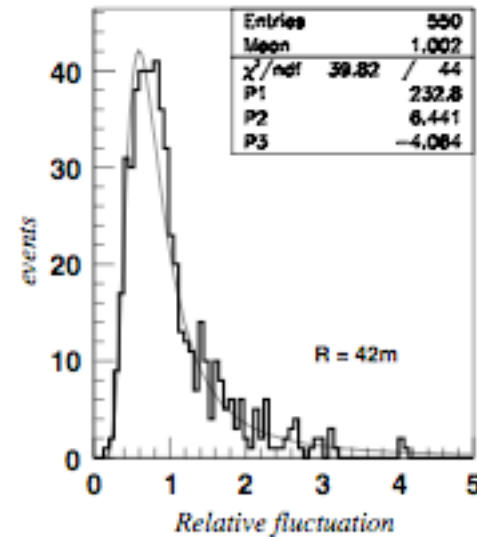
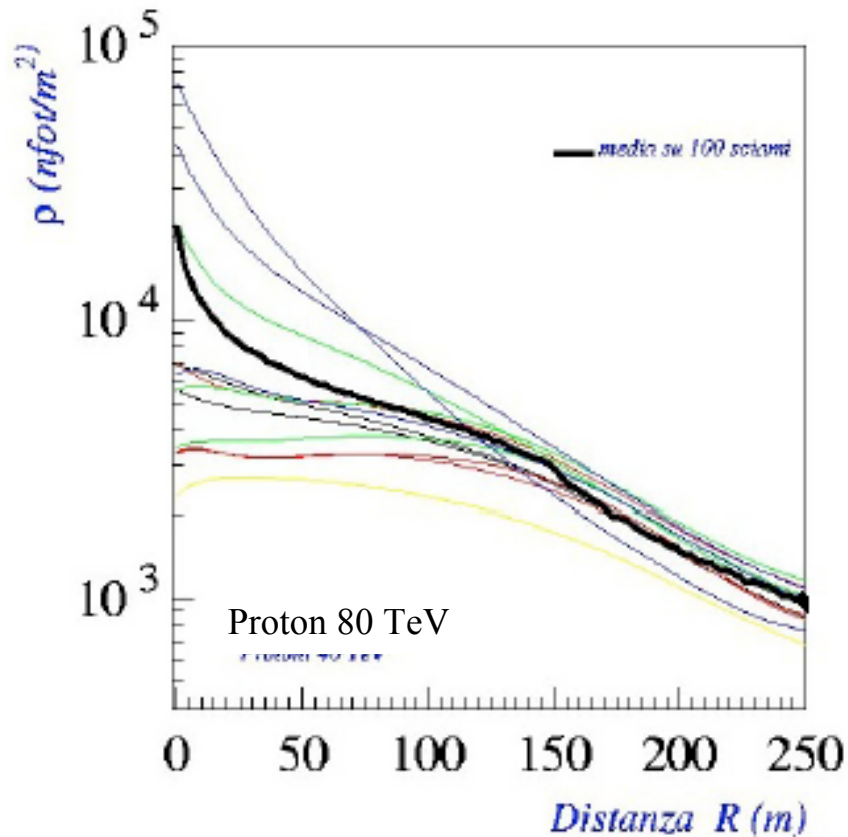
The beams are well defined:

- p at $E_0 < 40 \text{ TeV}$
- p+He at $40 < E_0 < 100 \text{ TeV}$
- p+He+CNO at $E_0 > 100 \text{ TeV}$

$$E \approx 80 \text{ TeV} \quad N_m^{\text{p}} \approx N_m^{\text{He}}$$

$$E \approx 250 \text{ TeV} \quad N_m^{\text{p}} \approx N_m^{\text{He}} \approx N_m^{\text{CNO}}$$

Same efficiency (inside 15%) in TeV μ production.



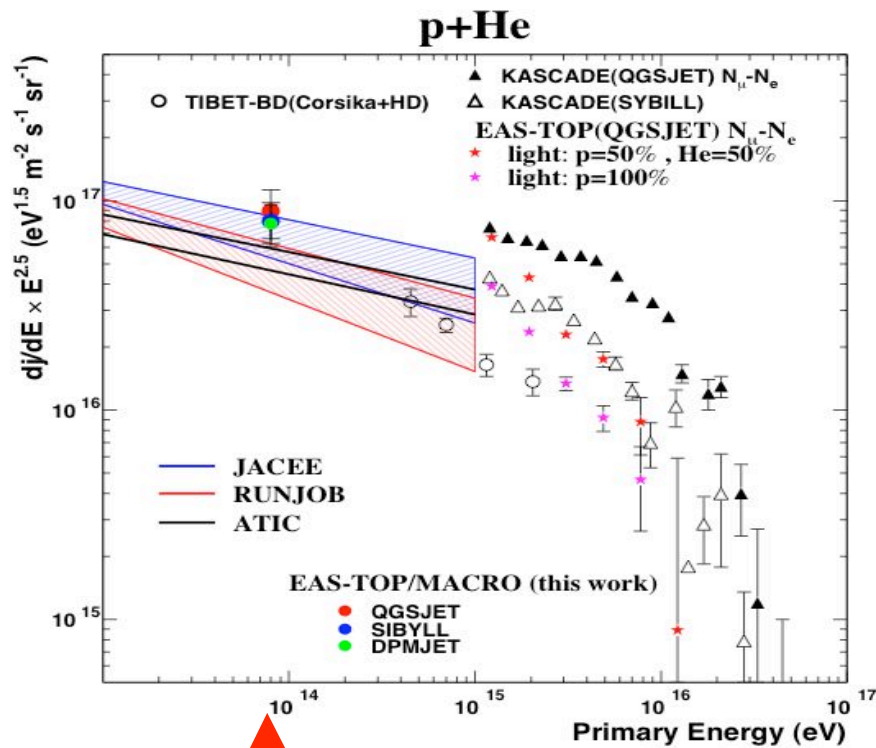
Photon density as a function
of core distance:

$r < 30$ m : γ density dominated by
fluctuations

$r = 30 - 140$ m: exp density, with slope
related to X_{max}

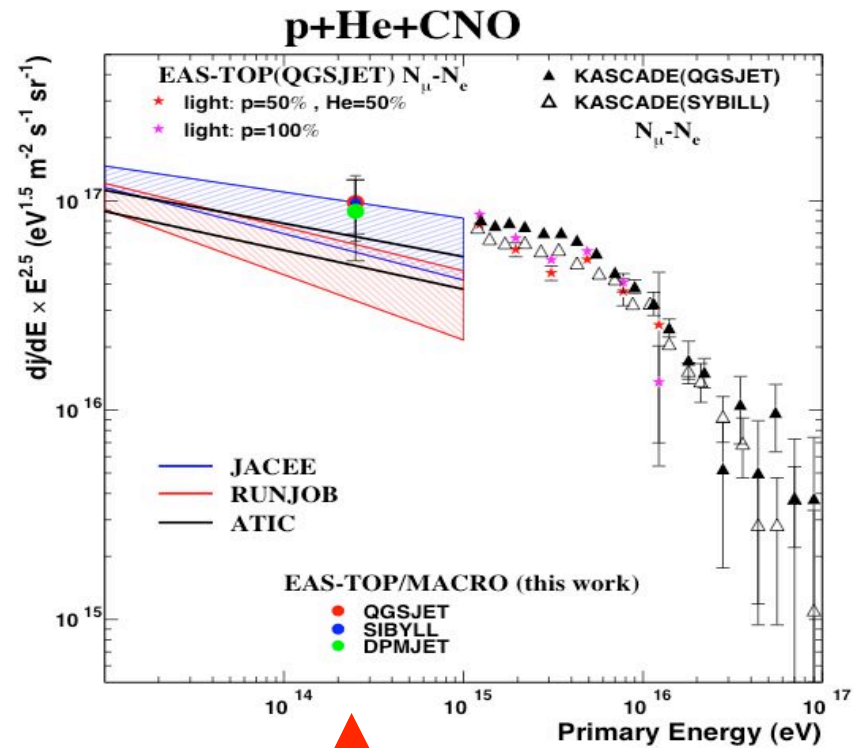
$r > 140$ m : almost constant light,
information on E_0

The Cerenkov photon density
for $r > 140$ m is a good
estimator of the primary
energy



$$J_p / J_{p+He} (80 \text{ TeV}) = (0.34 \pm 0.11)$$

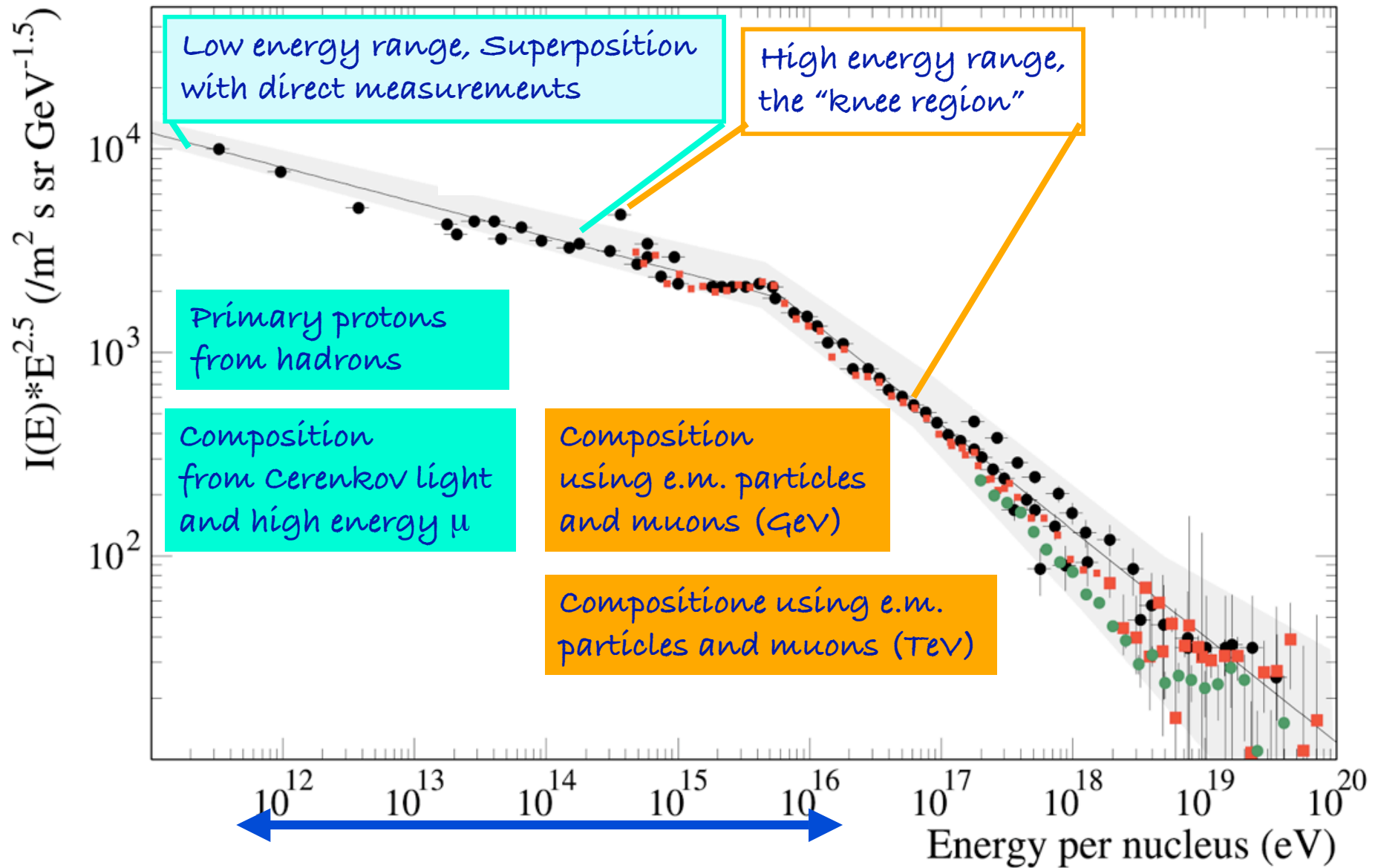
He dominates around 100 TeV
 CNO contribute significantly
 in the 100-1000 TeV region



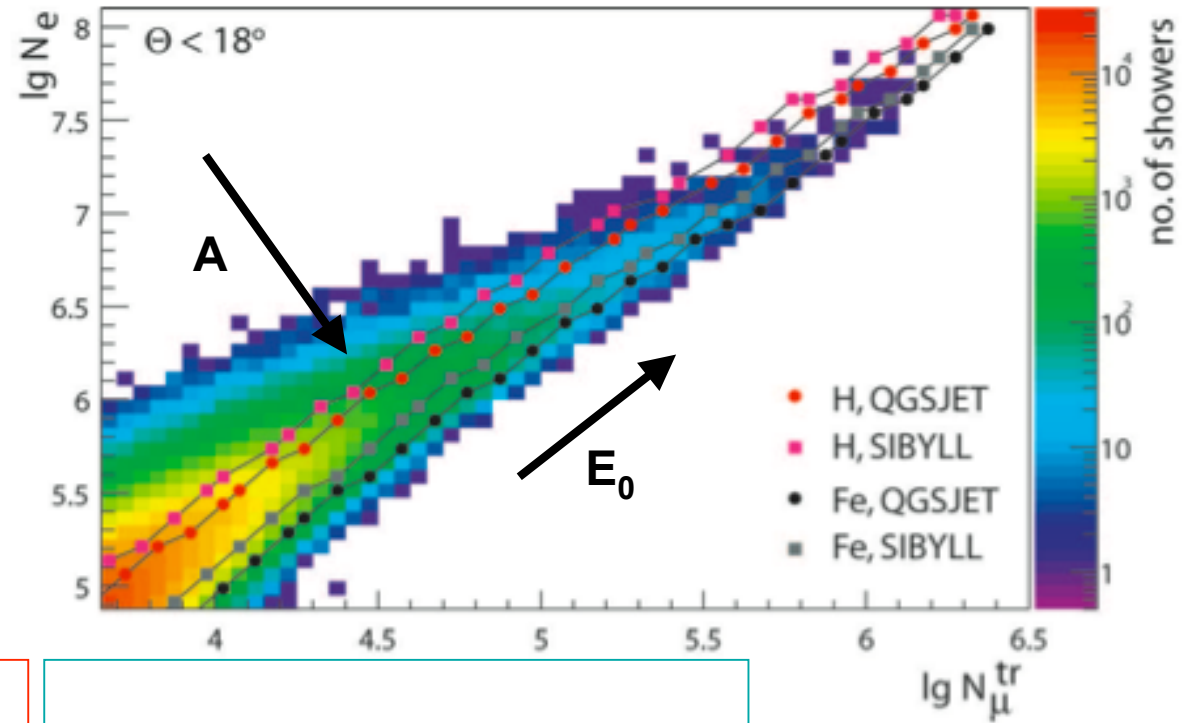
$$J_{p+He} / J_{p+He+CNO} (250 \text{ TeV}) = (0.73 \pm 0.18)$$

At 250 TeV: $J_p : J_{He} : J_{CNO}$
 $(0.21 \pm 0.09) : (0.52 \pm 0.19) : (0.27 \pm 0.18)$

Spectrum and Composition information



KASCADE:
From N_e, N_μ to E_0, A



$$\frac{dJ}{d \log N_e d \log N_\mu} = \sum_A \int_{-\infty}^{+\infty} \frac{dJ_A}{d \log E}$$

measured

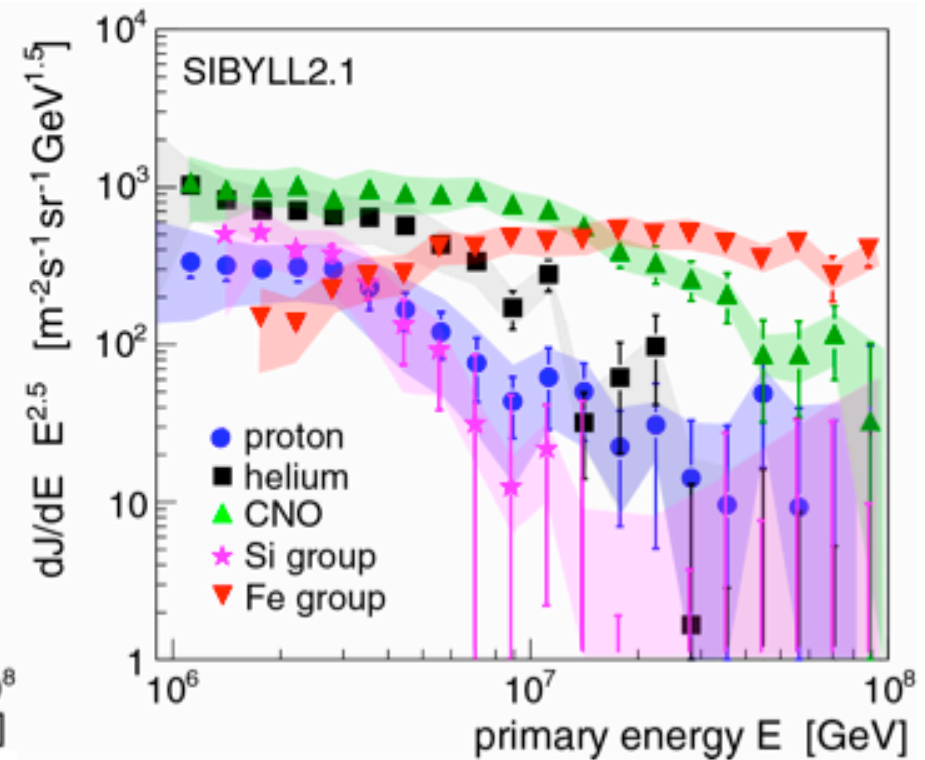
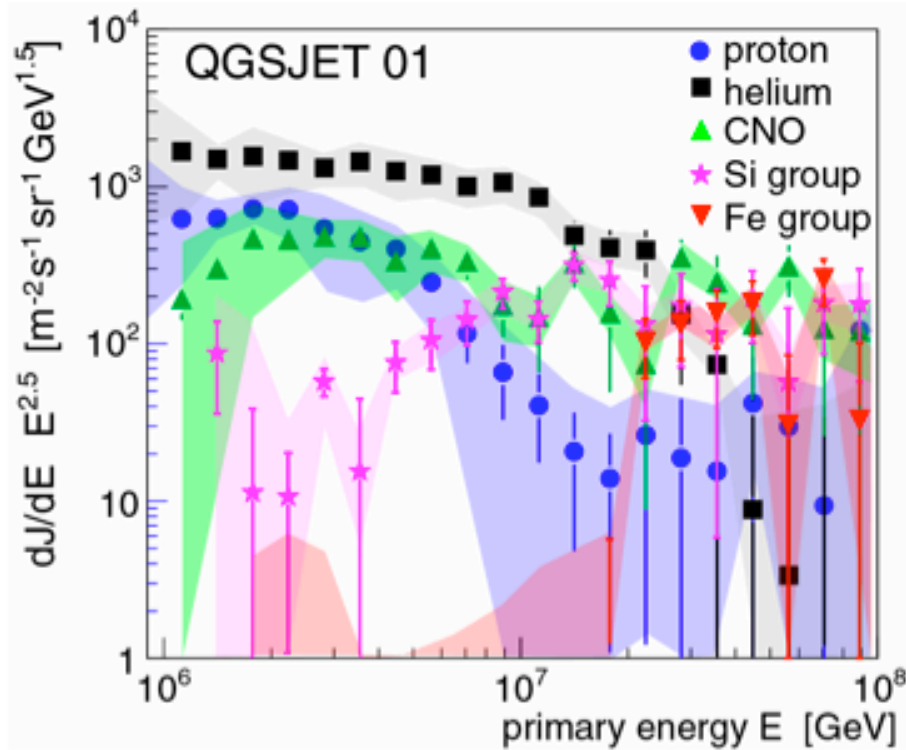
$$p_A(\log N_e, \log N_\mu | \log E) d \log E$$

Probability to get N_e, N_μ from a primary with (E_0, A)

$$p_A = \int_{-\infty}^{+\infty} \int_{-\infty}^{+\infty} s_{AE} r_A d \log N_e^{\text{true}} d \log N_\mu^{\text{tr, true}}$$

Intrinsic shower fluctuations

Trigger and Reconstruction efficiency
Reconstruction, resolution, systematics



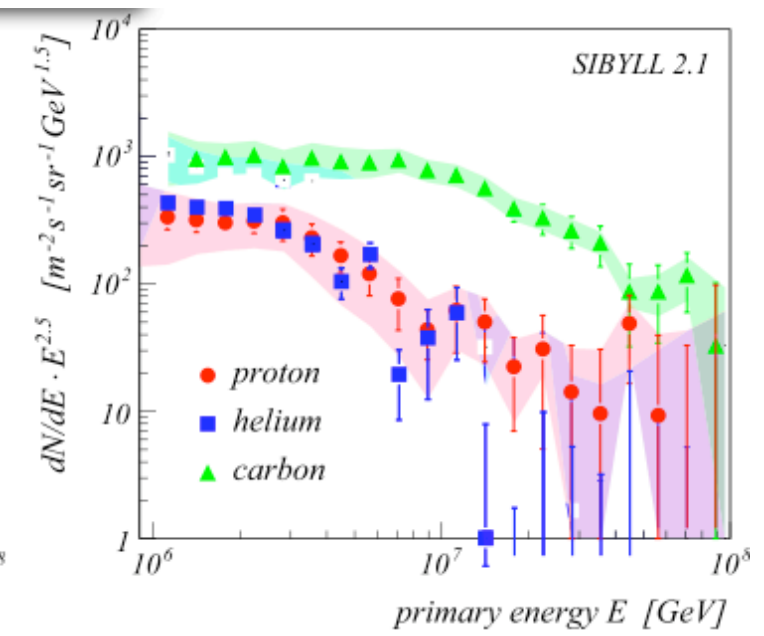
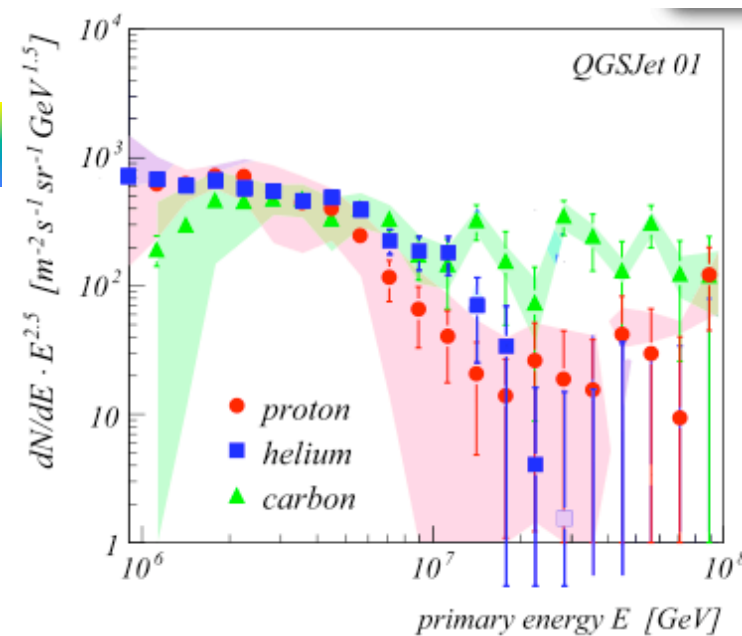
The knee is due to a cutoff in the light component
 The cutoff moves to higher energies for heavier nuclei

The interpretation is limited by knowledge of the properties
 of the hadronic interaction properties

[T.Antoni et al, Astrop.Phys. 24 (2005) 1]

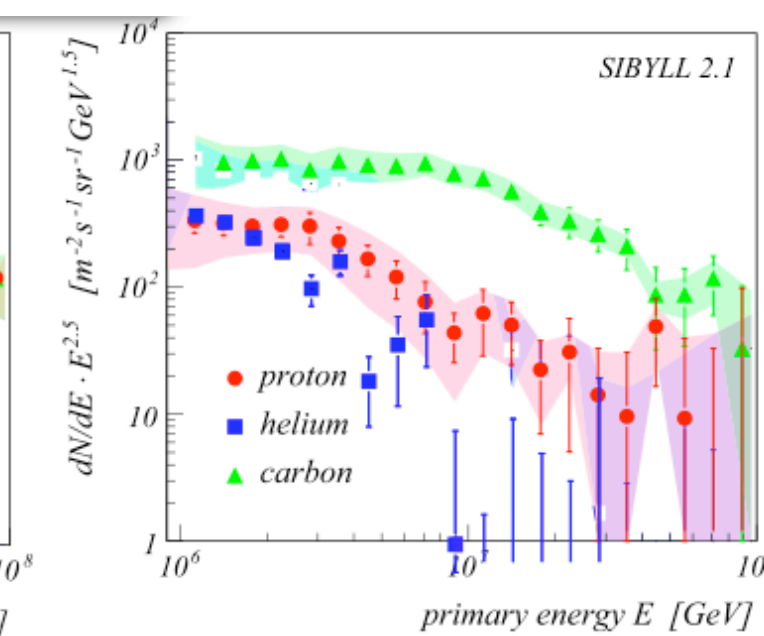
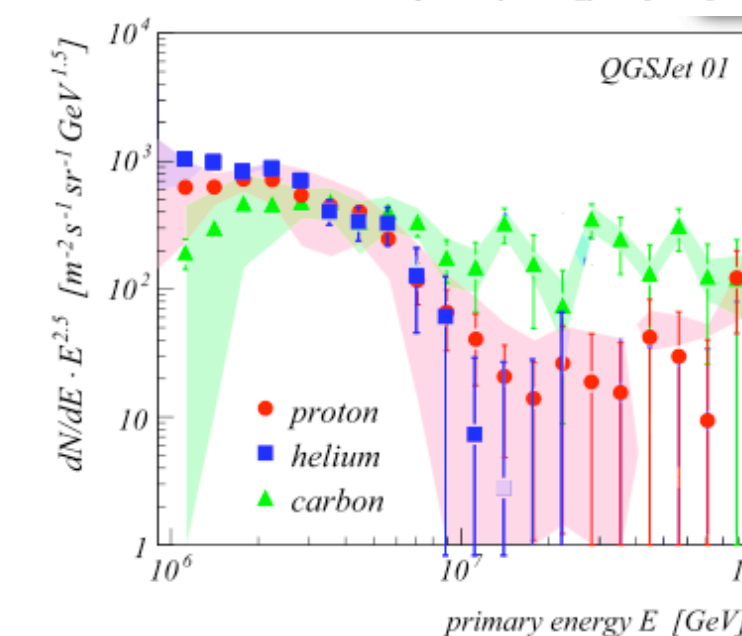
$$E_{\text{knee}}^A = Z E_{\text{knee}}^P$$

$$E_{\text{He}}/2$$

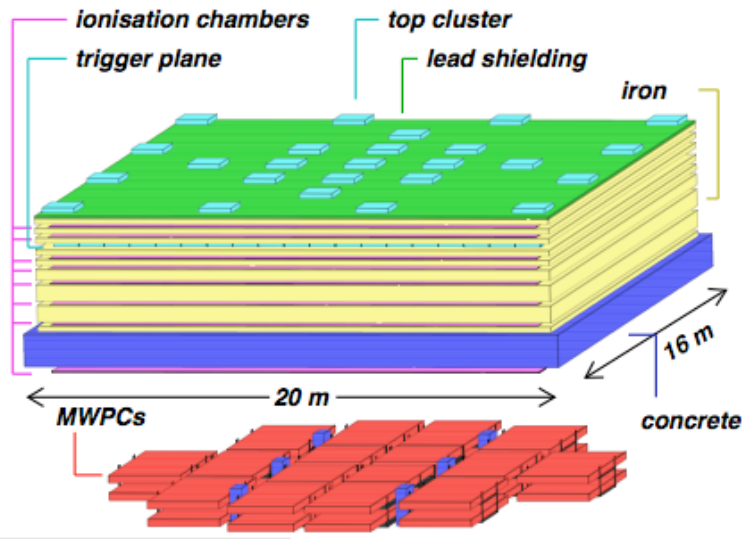


$$E_{\text{knee}}^A = A E_{\text{knee}}^P$$

$$E_{\text{He}}/4$$

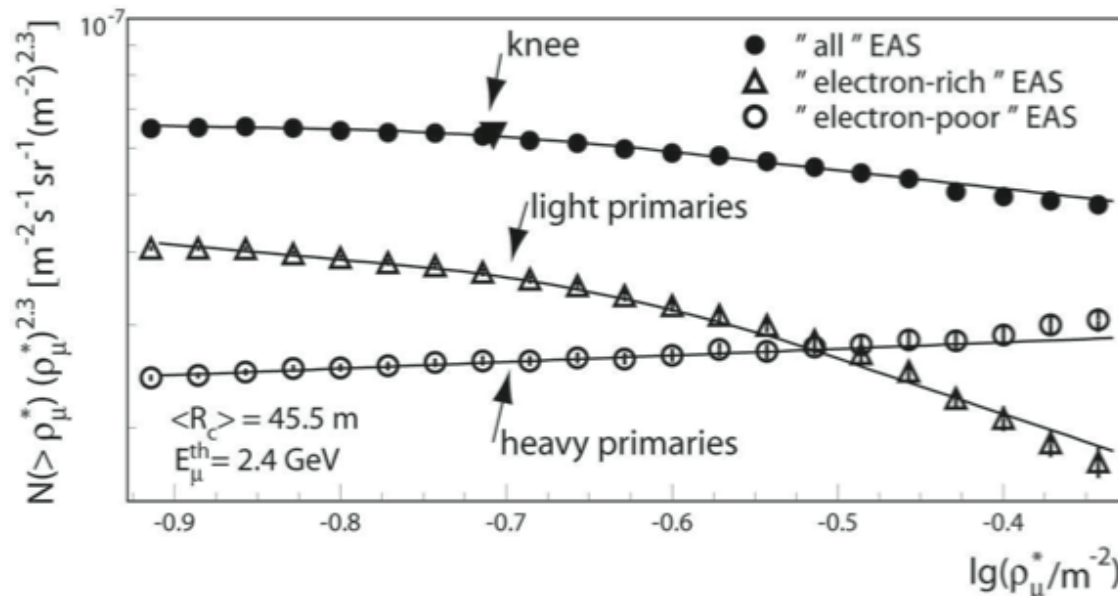


[K.H.Kampert, CRIS Conf. 2006]



The local muon density KASCADE

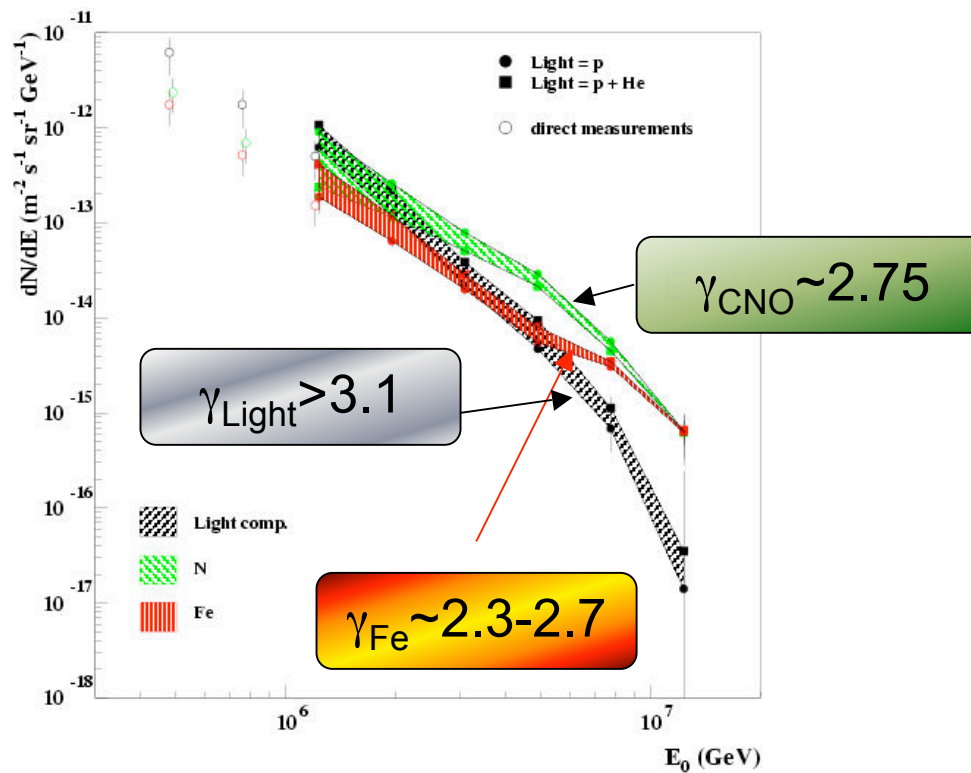
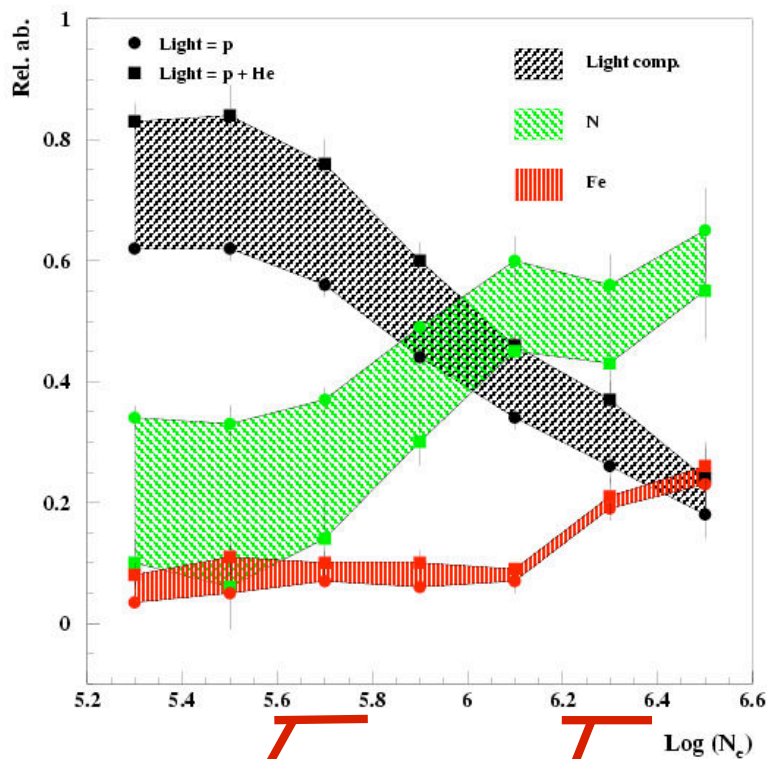
More direct approach, less dependent on interaction models



The knee is clearly seen in the light component only

[T. Antoni et al., Astrop. Phys., 16 (2002) 343]

EASTOP



Relative abundances

0.76 (p+He)
0.14 (N)
0.10 (Fe)

0.37 (p+He)
0.43 (N)
0.21 (Fe)

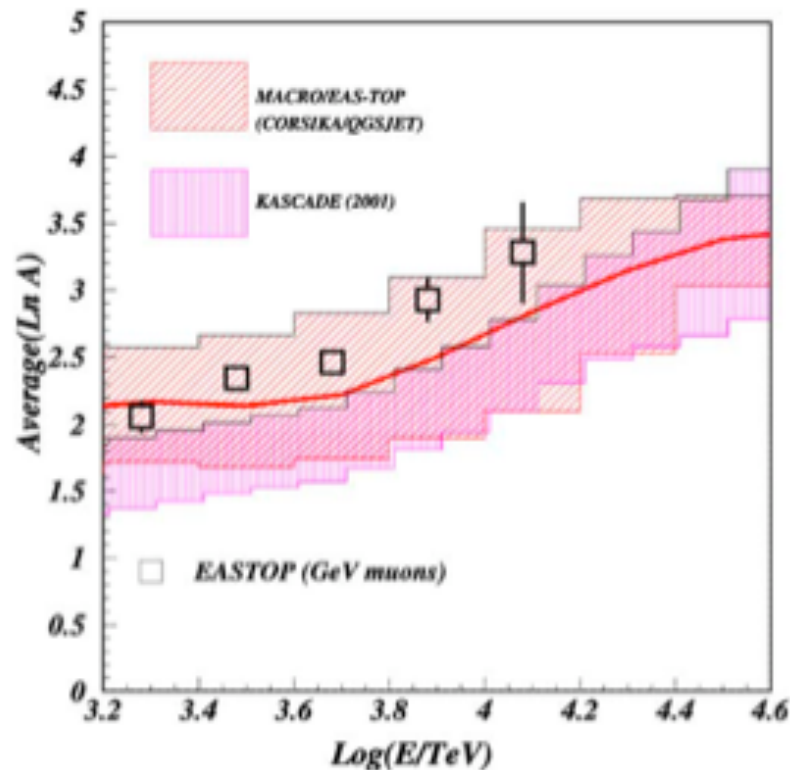
+ experimental size spectra
+ simulation

Energy spectra of each component

Composition from em and TeV muon data

EAS-TOP:
em size N_e
MACRO:
HE muons N_μ

Study of TeV muon multiplicity
distribution in different
intervals of N_e around the knee



increase in $\langle \ln A \rangle$ across the
knee
consistency of the model among
GeV and TeV muons



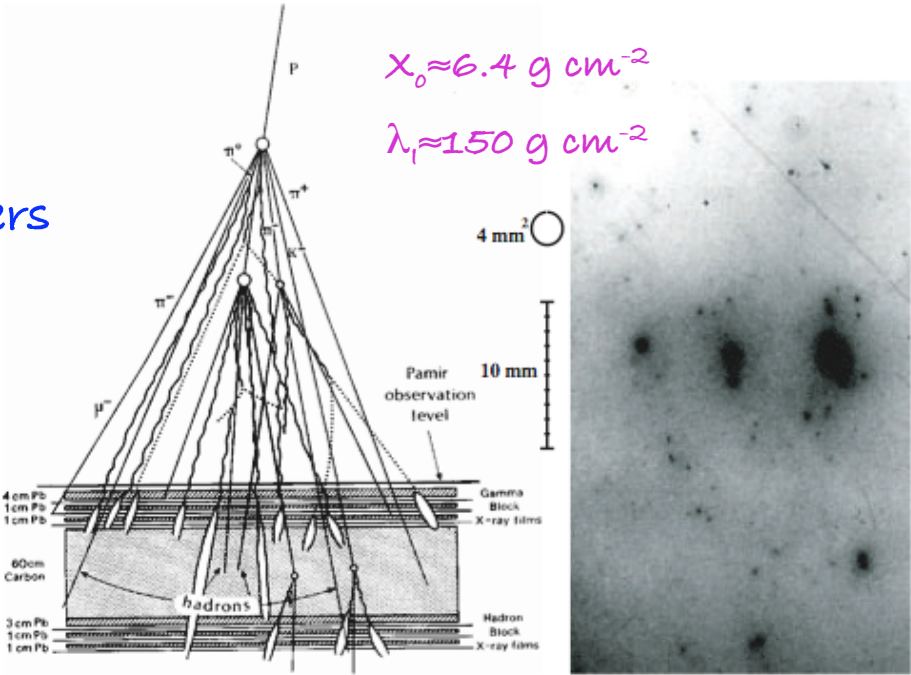
Tibet Yangbajing

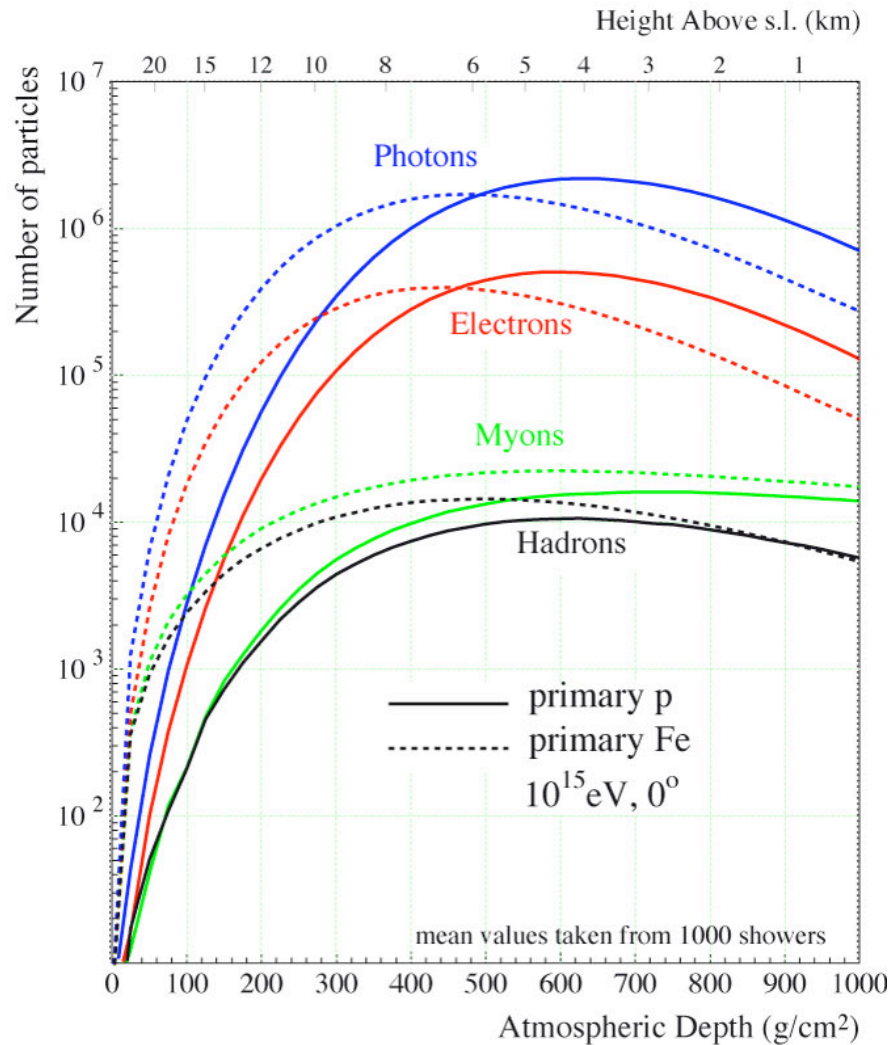
EAS array : 221 scintillation counters
 (15 m grid, $3.7 \cdot 10^4 \text{ m}^2$)
 + emulsion chambers (80 m^2)
 + burst detector (80 m^2)

4300 m asl (606 g cm^{-2})

Hybrid: sensitivity of EAS array
 Improved by with large emulsion chambers
 Enrich the proton and Helium events by
 tagging them with γ -families
 + very high altitude

Selection of primary protons
 event by event

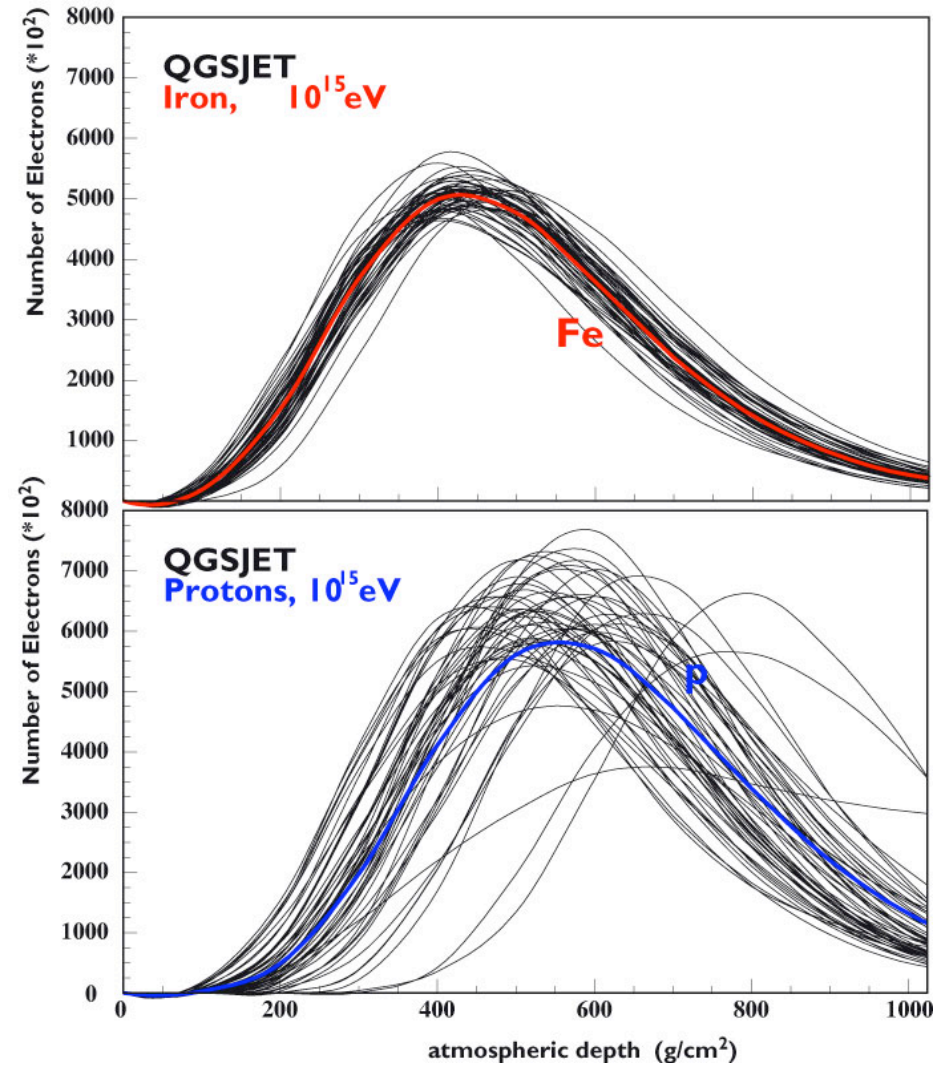




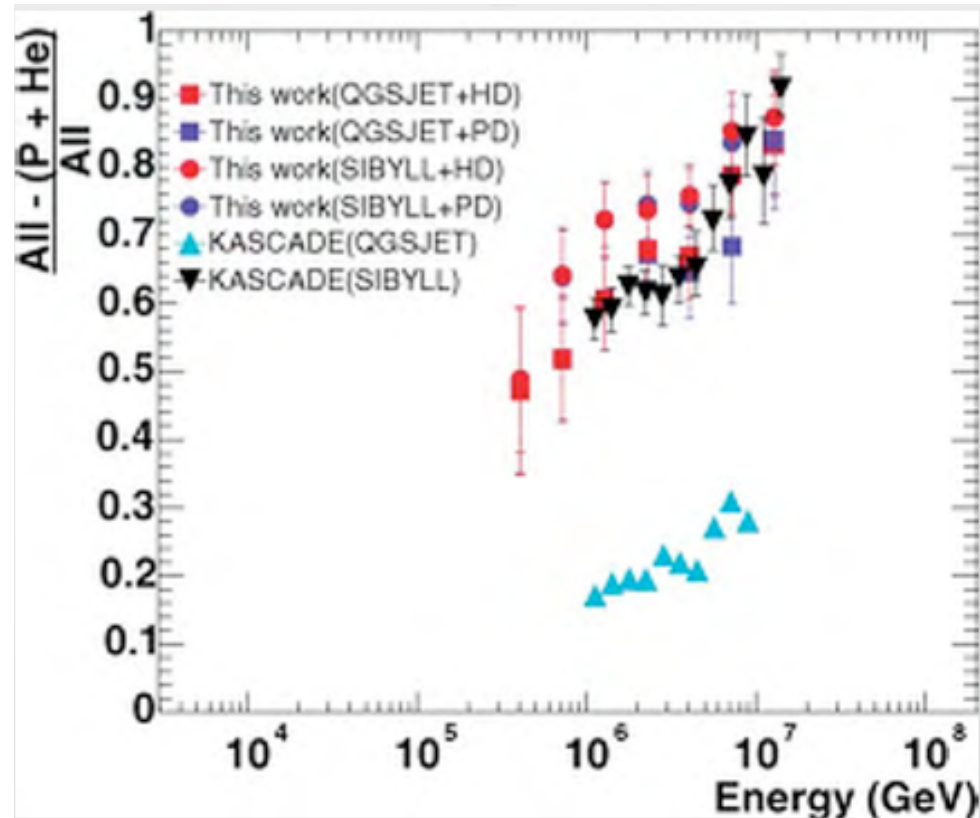
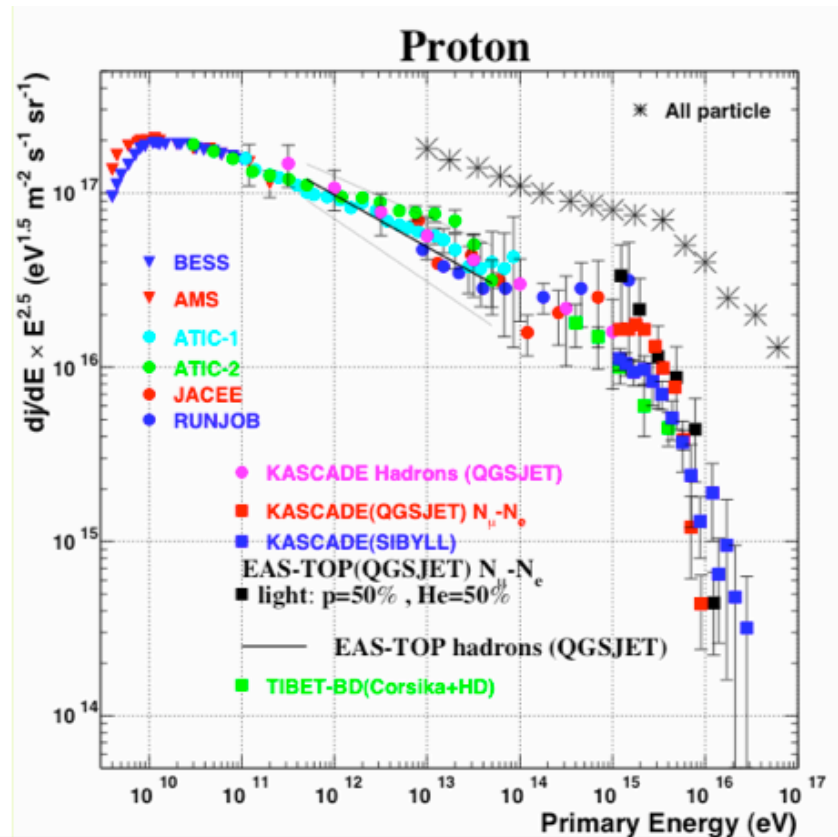
A primary Fe gives EAS with

- higher X_{max} [σ_{int} larger]
- more muons at ground
- less electrons at ground
- similar number of hadrons

The longitudinal development



Fluctuations are lower for EAS from heavy nuclei



TIBET results

p spectrum agrees with satellite and KASCADE(Sibyll)
 The knee in the all particle spectrum is due to nuclei
 Heavier than Helium
 Claim less dependence on models

but....

Knee assumed at 1.5 Z PeV very low and
 below the range of experiment
 Separation p/He : strong correlation errors on He spectrum
 Cannot see heavy nuclei

CASA-MIA

KNN TEST

Monte Carlo simulation and classification according to some "characteristics" : ρ_e , ρ_{μ} , S

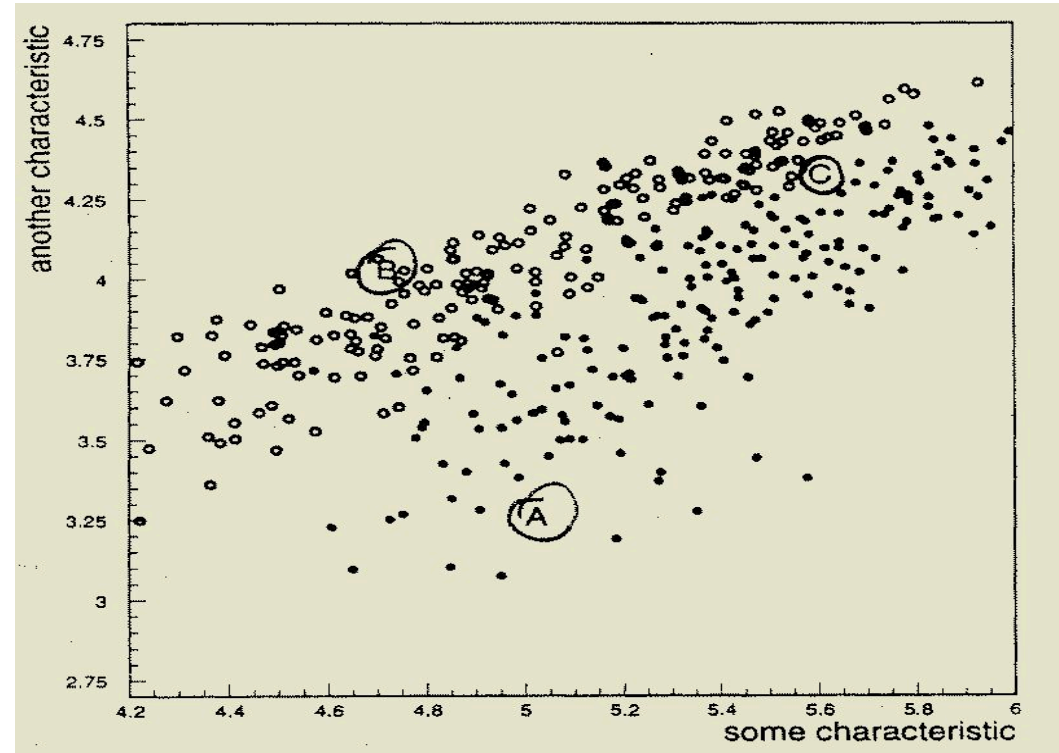
Each event is assigned a "class" in the plane of "characteristics"

K nearest neighbor:

event A : 100% class 1

event B : 100% class 2

event C : 50% - 50%

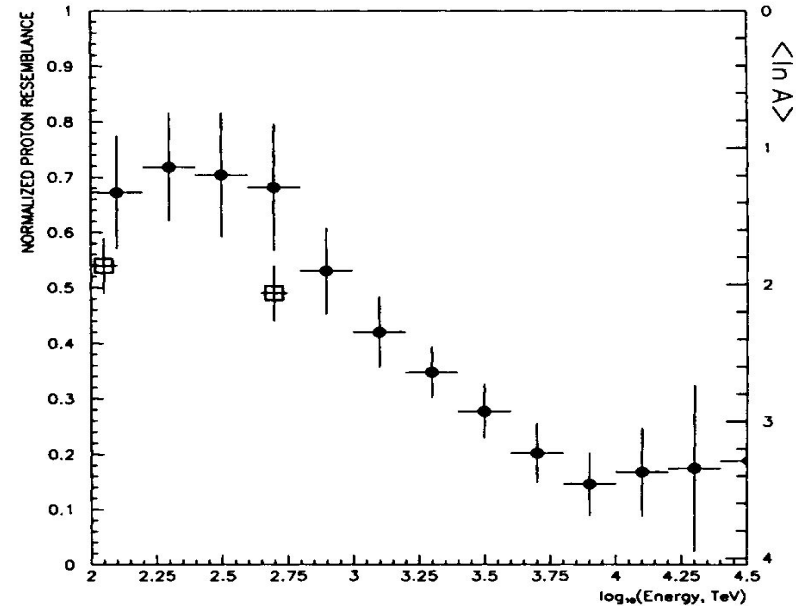


Fluctuations tend to superimpose classes:
only "p-like" and "Fe-like" events

Proton resemblance plot

average fraction of 5NN
protons

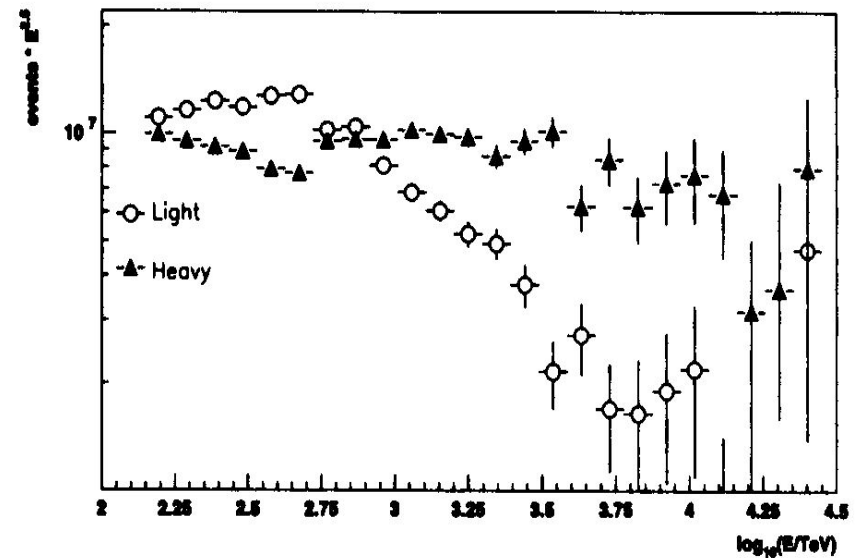
- ✓ Heavier composition above the knee
- ✓ no model dependence



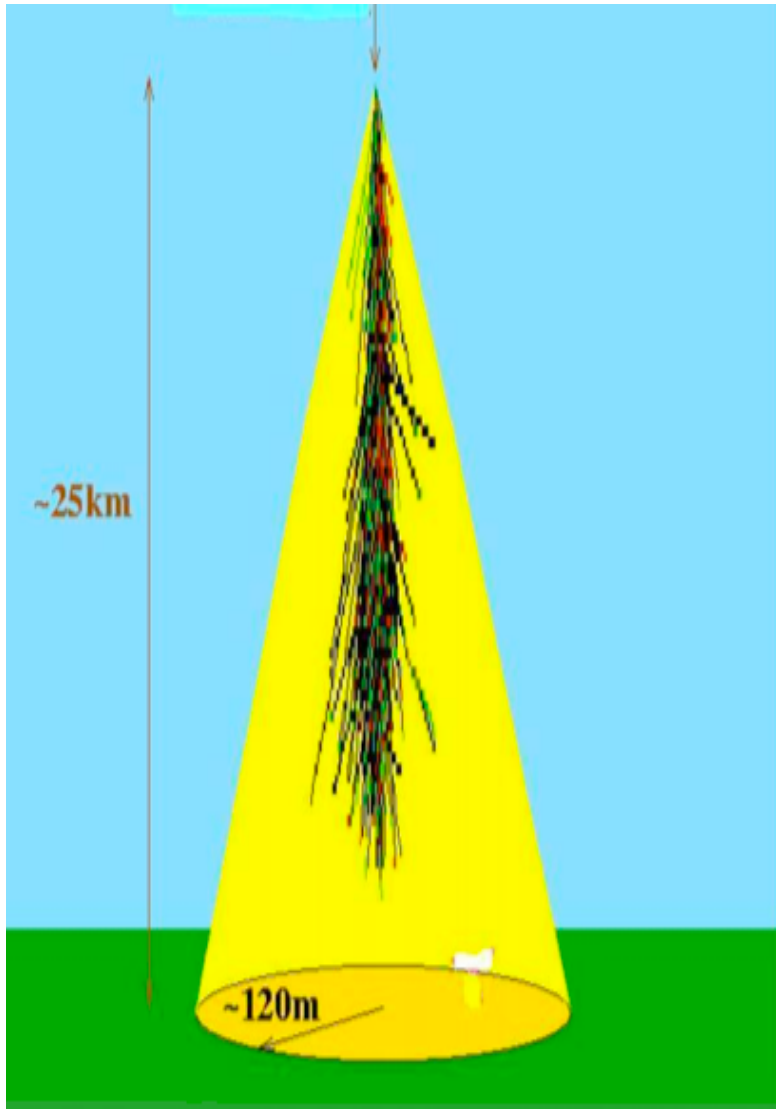
Consistency check

p-like events if $>50\%$ 5NN protons
Fe-like if less

- ✓ composition heavier above the knee
- ✓ bend due to light component
- ✓ not enough statistics to see the bend in the heavy one



Using Cerenkov detectors...



High photon number density



Higher signal-to-noise ratio with arrays with smaller area or larger separation

Smaller absorption of γ in atmosphere

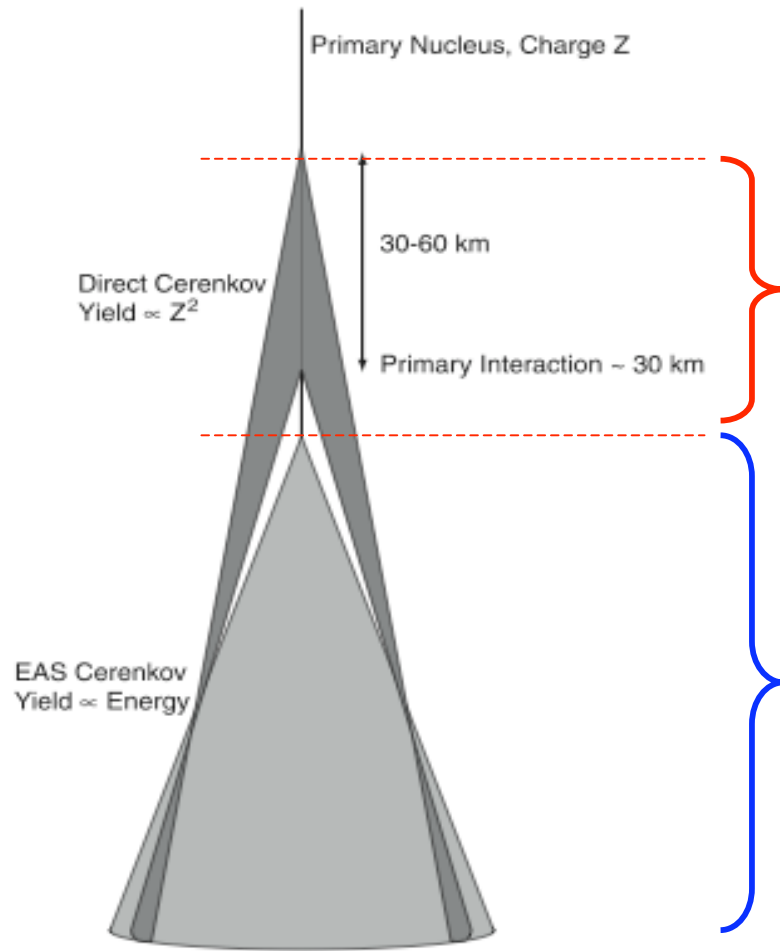


Broader lateral distribution

Only moonless nights



Low duty cycle



Direct emission by the primary particle

Yield $\propto Z^2$

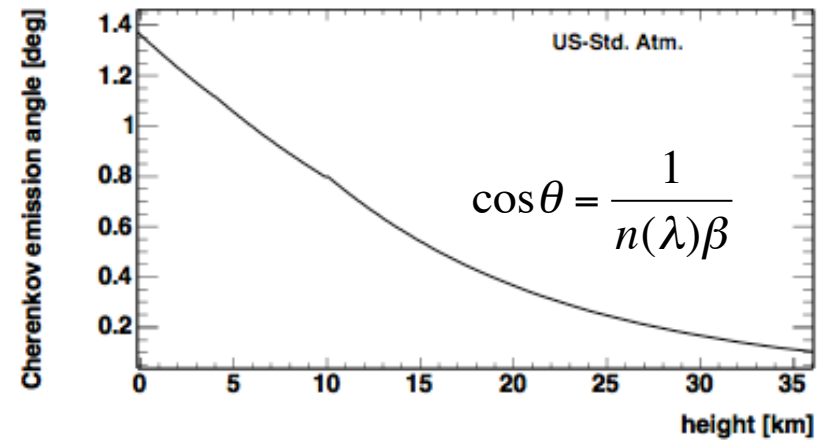
E_{\max} detectable : $C_{EAS} \sim C_{DIR}$

Emission angle $0.15^\circ - 0.3^\circ$

Cerenkov emission by EAS particles

Yield $\propto E^2$

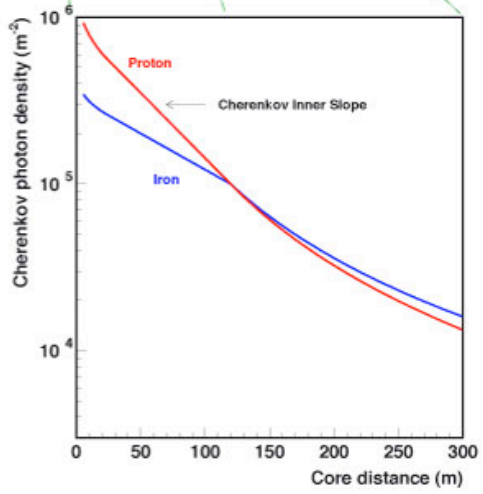
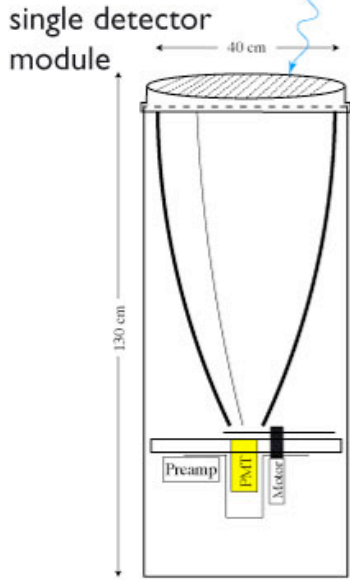
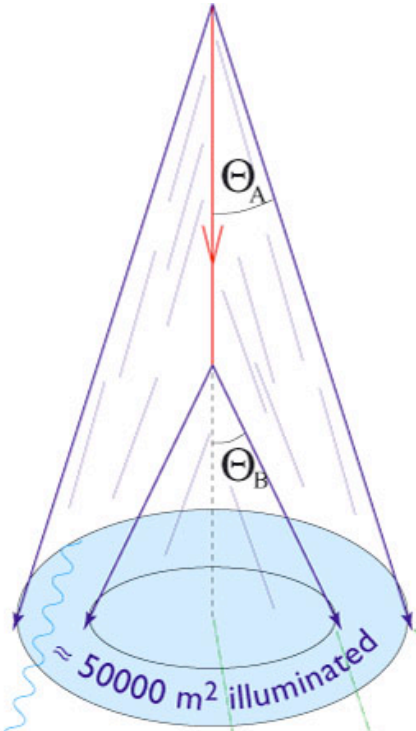
Emission angle $> 1^\circ$



(I) Wide-angle Cerenkov detectors

Idea: sampling the Cerenkov lateral distribution, which is a superposition of the light generated at all heights

Characteristic ring of light at $\approx 100-150$ m from core



$$C(r) = C_{120} (r/120)^{-\beta} \quad r=120-350 \text{ m}$$

$$C(r) = C_{120} e^{-sr} \quad r < 120 \text{ m}$$

Inner Slope $\propto X_{max}$
MASS

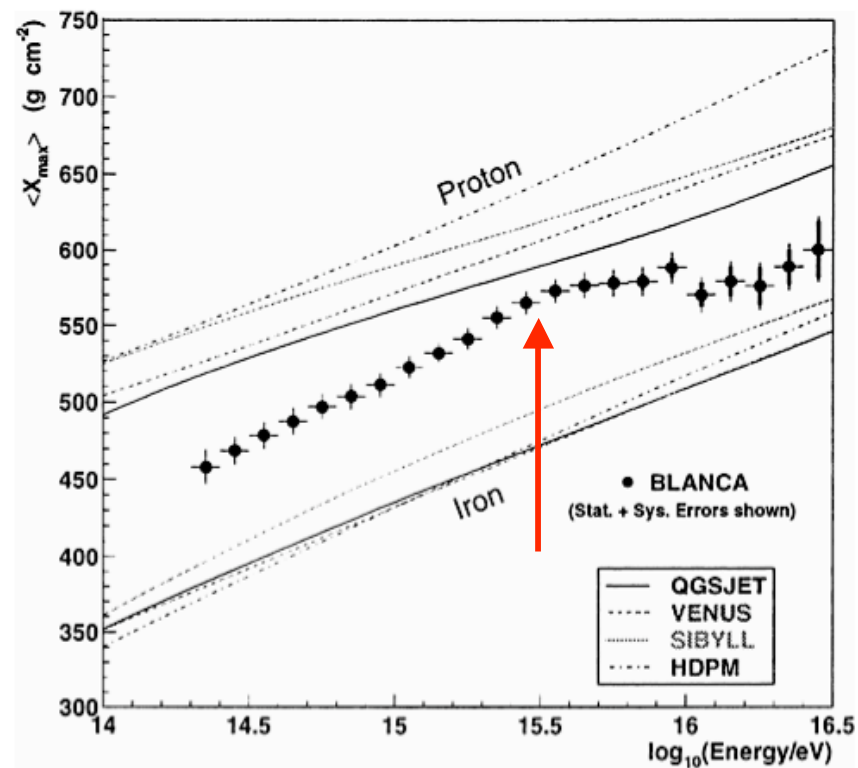
Intensity at 120 m
 $C_{120} \propto \text{Energy}$

BLANCA — 144 angle integrating detectors

$\langle X_{\max} \rangle$ derived directly from the slope of the Cerenkov ldf (through MC)

weak dependence on model: *mixed composition lighter approaching the knee, then heavier*

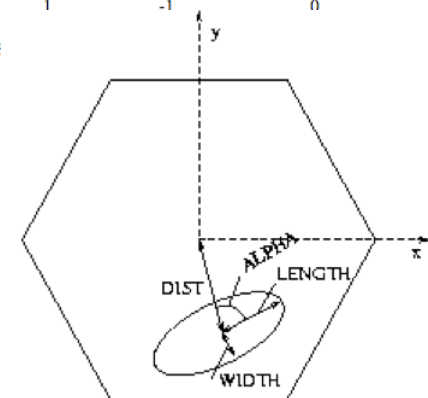
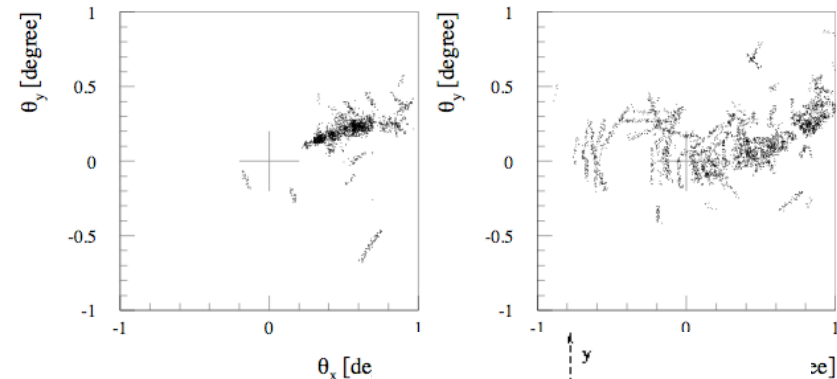
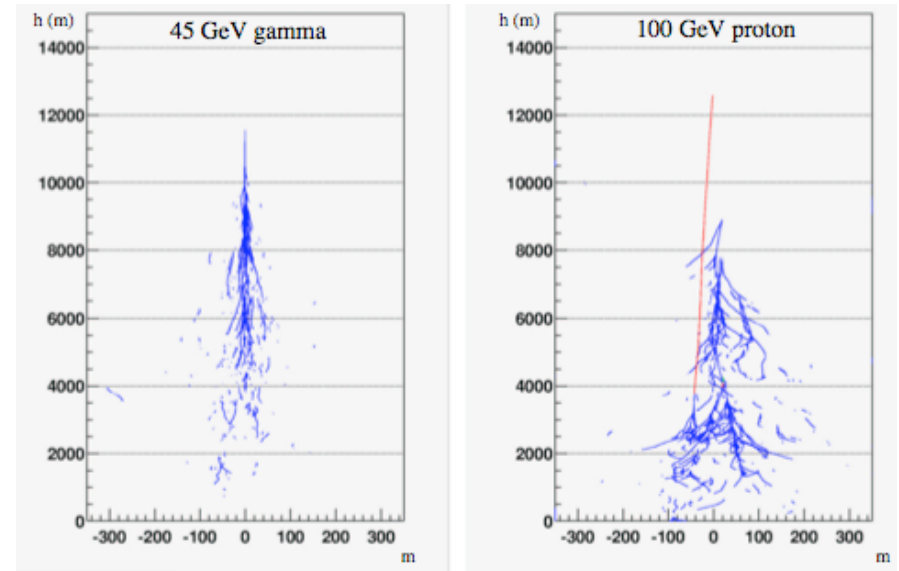
systematic uncertainty $<10\%$ in the whole range

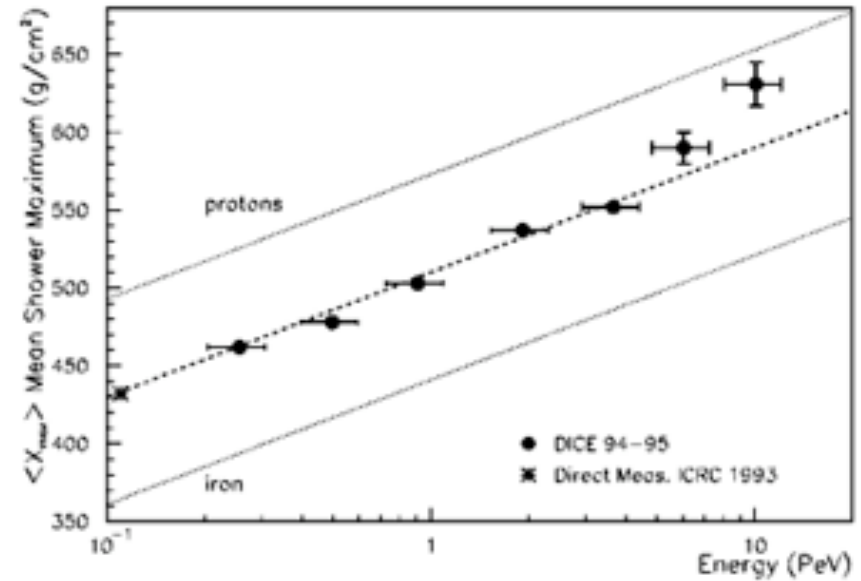
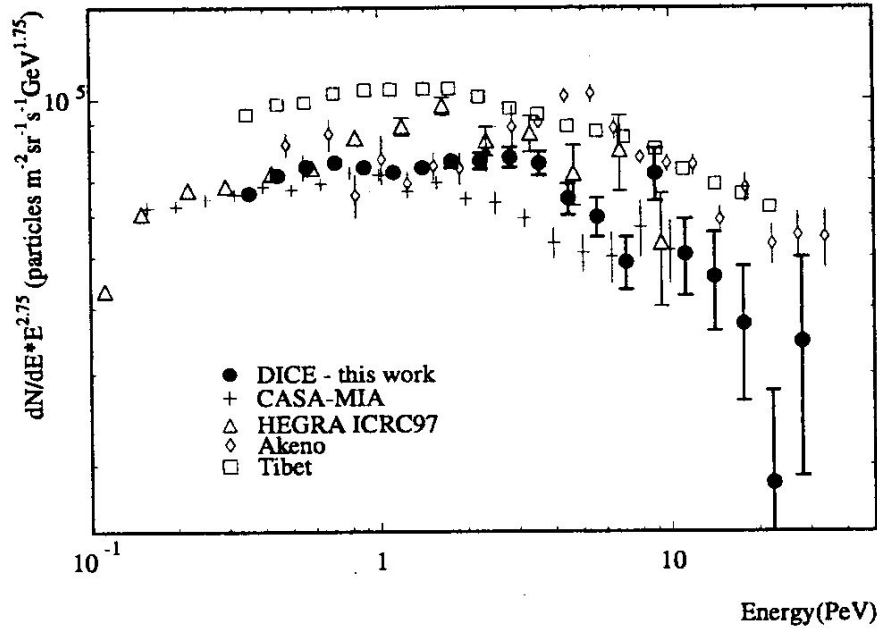


[J.W.Fowler et al, Astrop.Phys.15 (2001) 49]

(II) Imaging Cerenkov detectors

- (i) CR within the field of view produces an image of the shower on the focal plane
- (ii) Need to know
 - from EAS array
 - distance to core and shower direction
 - from Monte Carlo
 - the Cerenkov light distr. around the axis at each depth
- (iii) Fit to the Longitudinal distribution
 - ↪ X_{max} , N_{γ} and width
- (iv) Total intensity of Cerenkov light
 - ↪ E from total intensity of C light

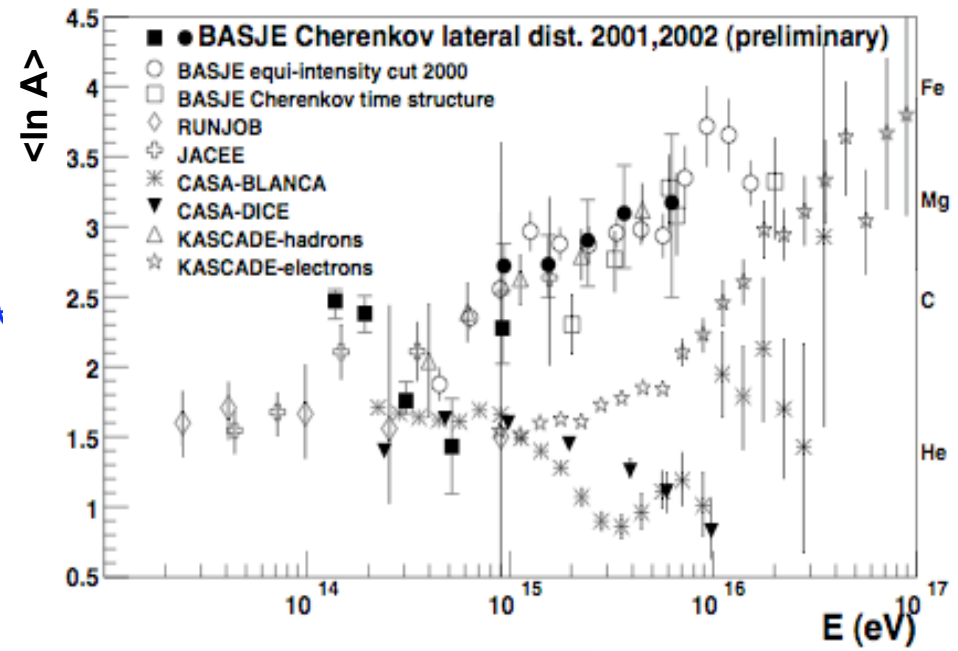




DICE – 2 Cerenkov imaging telescopes

Knee near 3 PeV, smooth change

Composition in agreement with BLANCA



(III) Direct Cerenkov detection by IACT

Before the first interaction...

$\delta(h) = (n-1)$, n =local atmosphere refraction index

$$N_c \propto Z^2 \left(\frac{1}{\gamma_{thr}^2} - \frac{1}{\gamma^2} \right) \quad \text{Cerenkov emission rate}$$

$$\gamma_{thr} \approx \frac{1}{\sqrt{2\delta(h)}}$$



$$E_{MIN}(h) \approx \frac{mc^2}{\sqrt{2\delta(h)}}$$

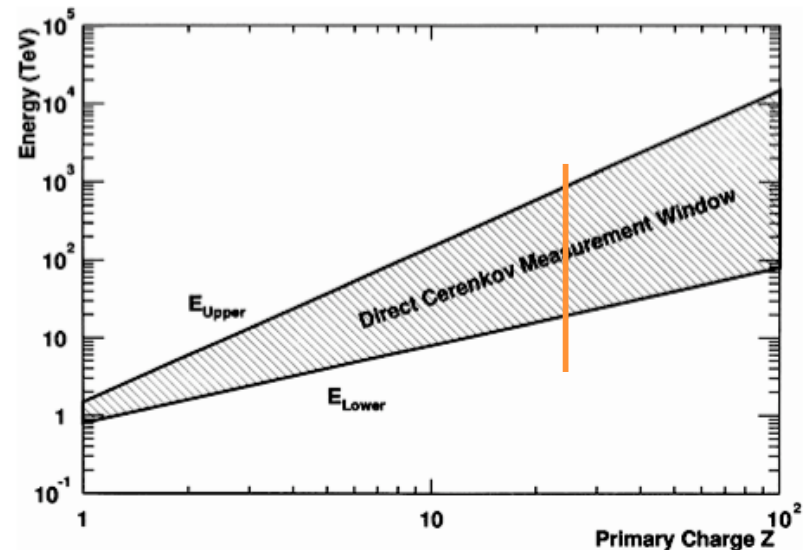
E.g. Fe nucleus: At sea level $\gamma_{thr} \sim 42$ $E_{thr} \sim 2$ TeV
 At 50 km $\gamma_{thr} \sim 680$ $E_{thr} \sim 36$ TeV

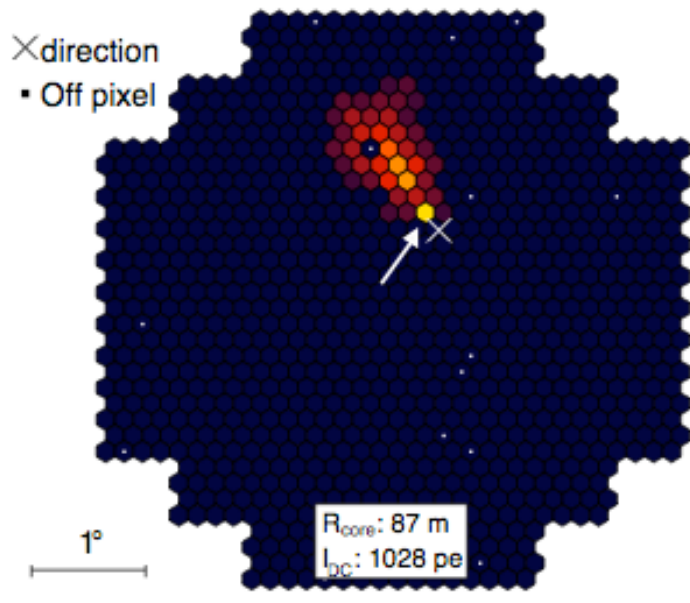
$$Y_{DIR} \approx Y_{EAS}$$



$$E_{MAX}$$

$$\Delta E/E \propto Z$$





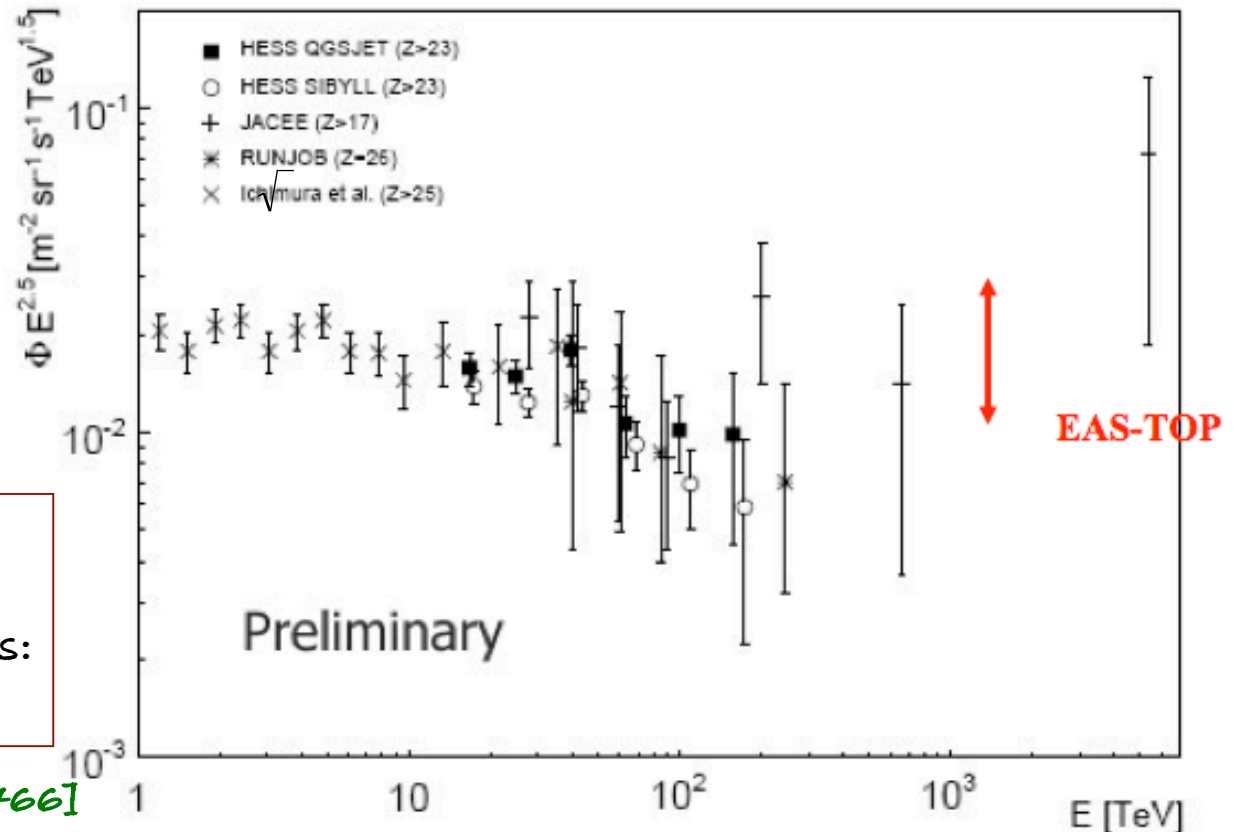
HESS IACT - direct Cerenkov

C_{DIR} separated by IACT as a single high intensity pixel between the reconstructed EAS direction and the centre of gravity of the shower
 pixel size = 0.1°

E from total intensity of image ($E_{thr} = 13$ TeV)

$$Z = \sqrt{I_{DC}}$$

Increase in statistics
 increase energy range
 Good agreement with others:
 more precise



[F.Aharonian et al., astro-ph/0701766]

Summary on spectrum and composition

Type	Technique	Energy Range	Experiment and Sensitive Components
dir.	Spectrometer	1-200 GeV	AMS(p-He), BESS(p,He), HEAO(CNO-Fe)
dir.	Calorimeter	30GeV - 500 TeV	ATIC(all), CREAM(all)
dir.	Emulsion chambers	10-500 TeV	JACEE, RUNJOB (all)
ind.	Hadron calorimeter	500 GeV -1 PeV	KASCADE, EAS-TOP (p)
ind.	Muon spectrometer	100 GeV - 10 TeV	L3+C(mostly p and He)
ind.	Cherenkov + TeV μ	50-300 TeV	EAS-TOP/MACRO(p,He,CNO)
ind.	N_e-N_μ	100 TeV - 10 PeV	GRAPES, KASCADE, EAS-TOP (all)
ind.	Emulsion chambers	5-300 TeV	Tibet AS γ (p,He)

The spectra from direct and EAS measurements in the “low” energy region do agree quite well

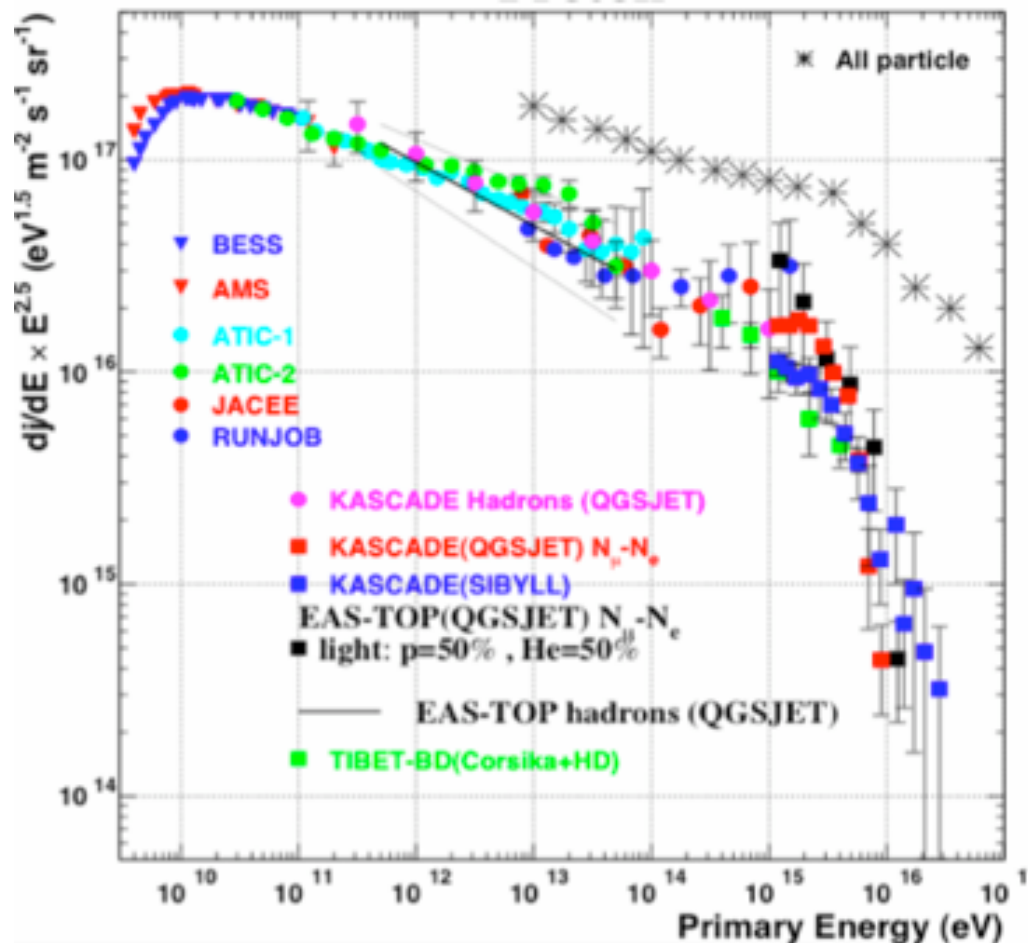
The knee in the all particle spectrum exists at 3-4 PeV

The knee of the cr spectrum is most probably due to light elements (He); the mean composition gets heavier above the knee.

Does the knee scale as E/Z or as E/A ? Uncertain...

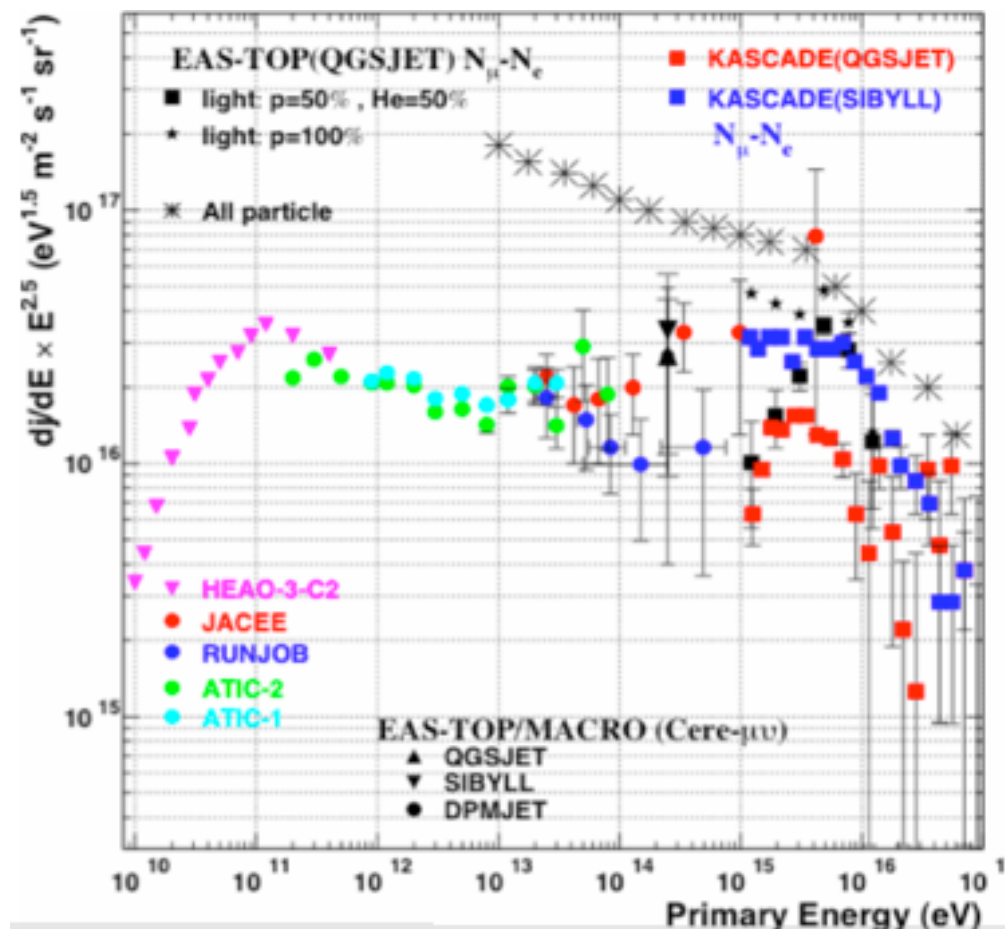
Hadronic interaction models are the main source of systematics

The proton spectrum



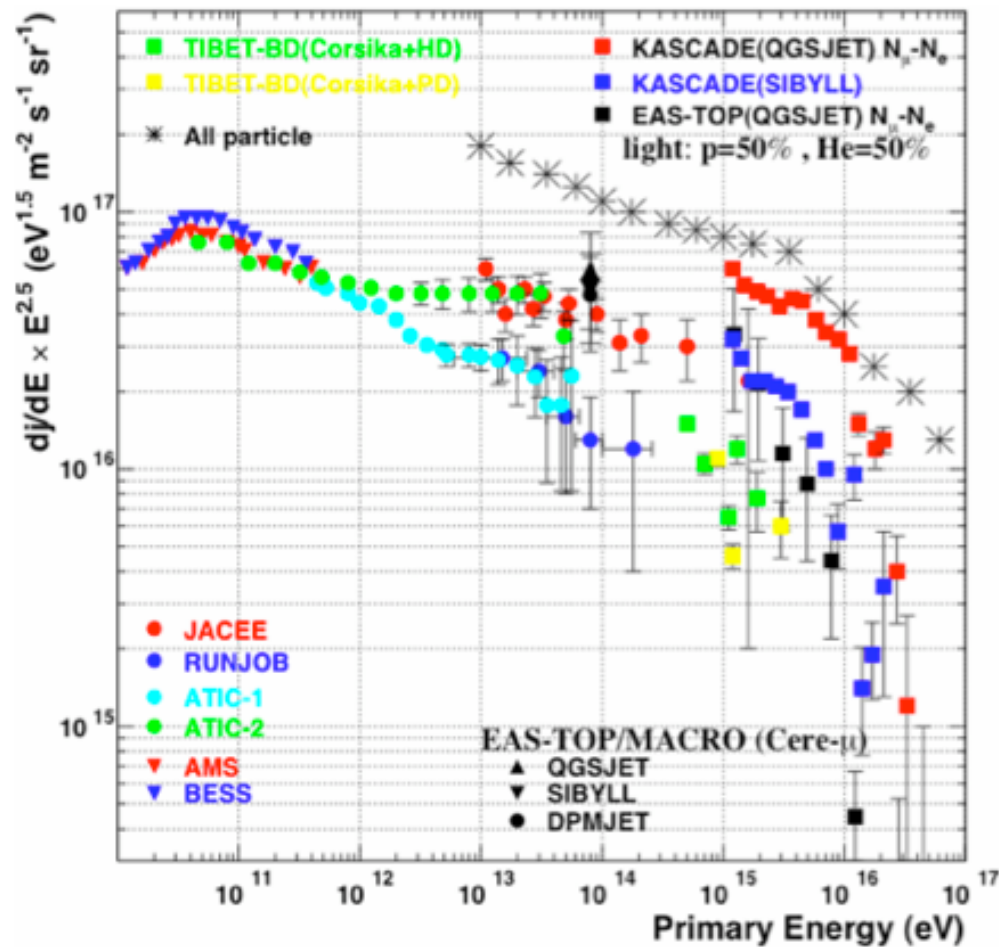
Good agreement for all measurements
 Global fit to the spectrum $dN/dE \propto E^{-2.75}$

The Helium spectrum

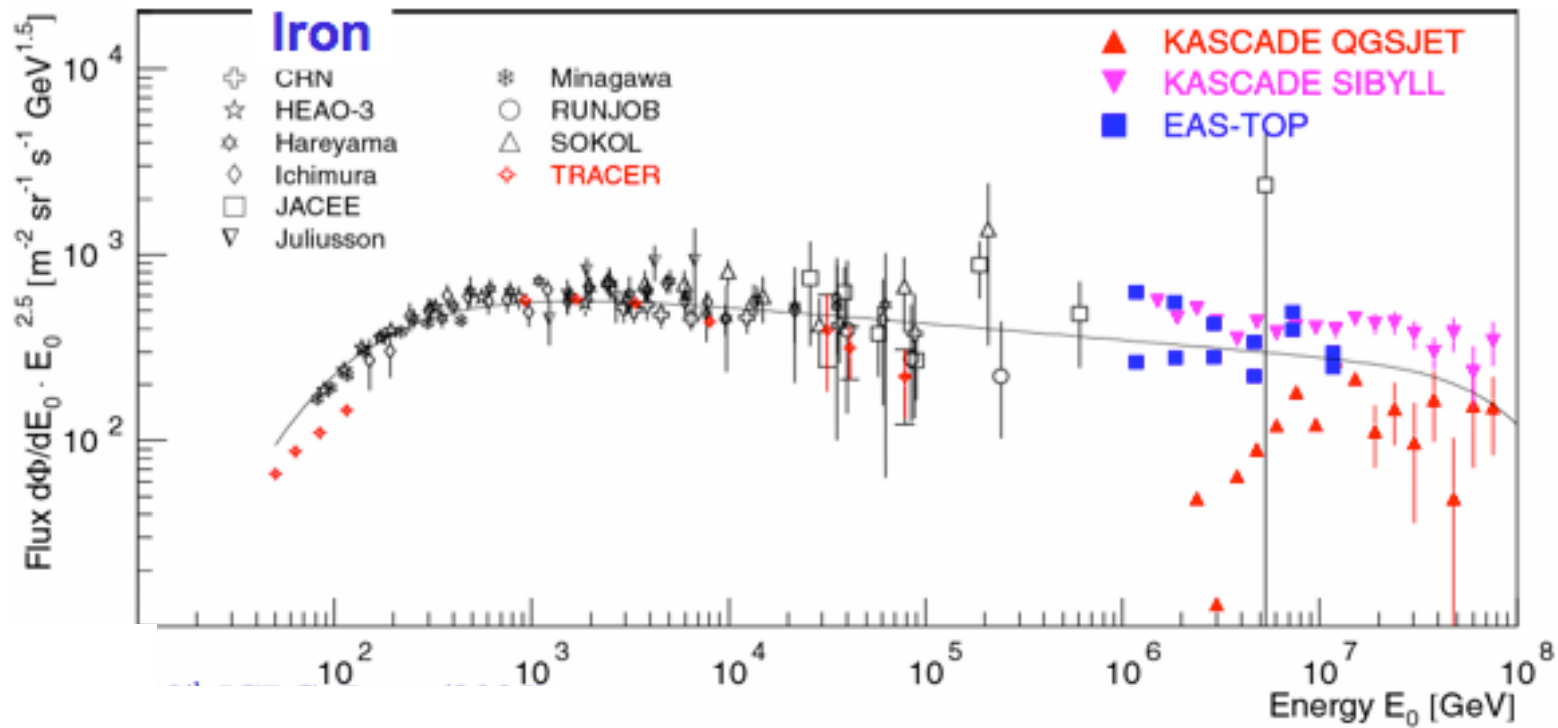


Discrepancy between Jacee and Runjob results: ATIC2 agrees with Jacee
 Global fit to the spectrum $dN/dE \propto E^{-2.61}$
 Accuracy for the $N_e - N_\mu$ results ~ direct measurements

The CNO spectrum

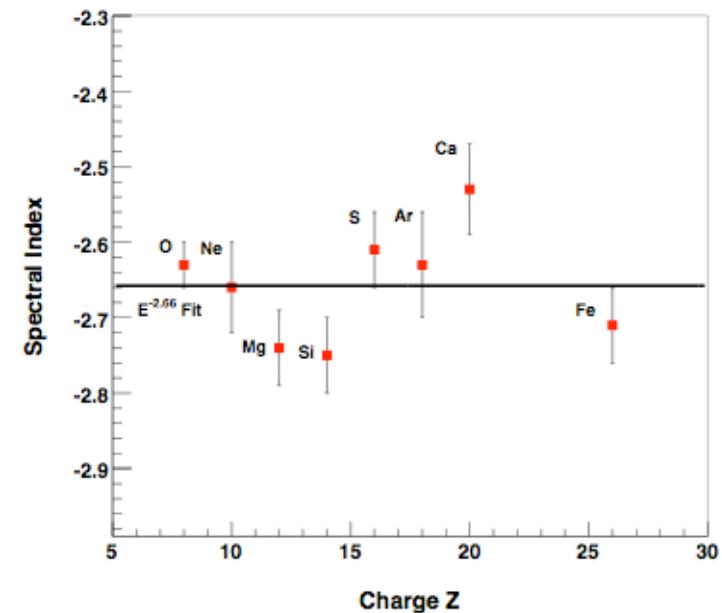


Different definitions of CNO group
 Global fit to the spectrum $dN/dE \propto E^{-2.61}$



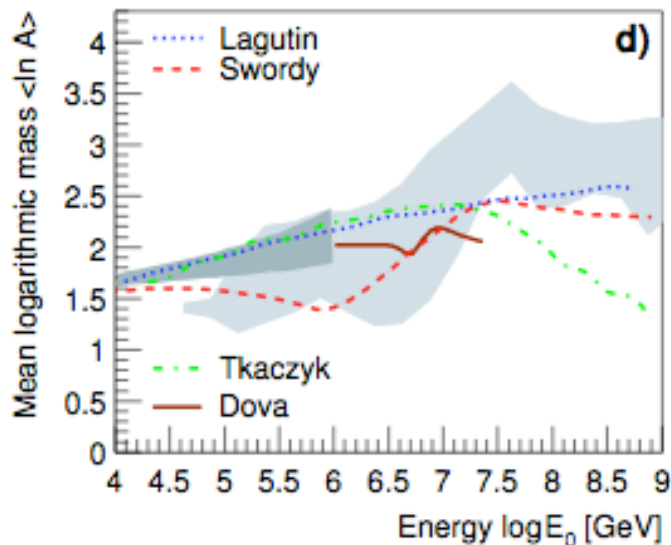
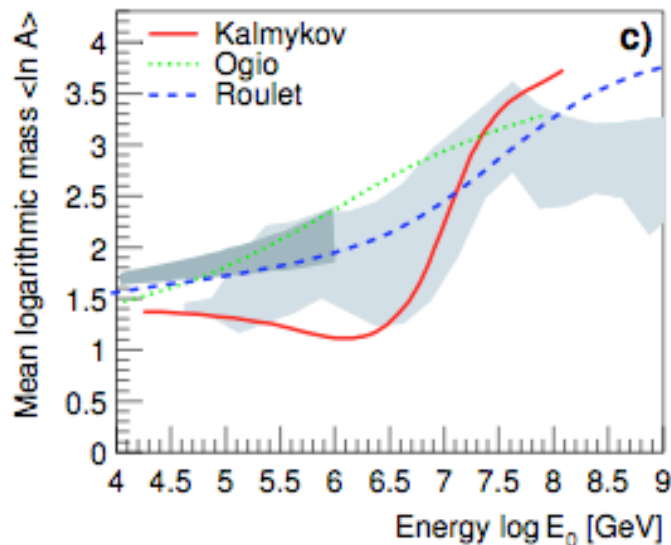
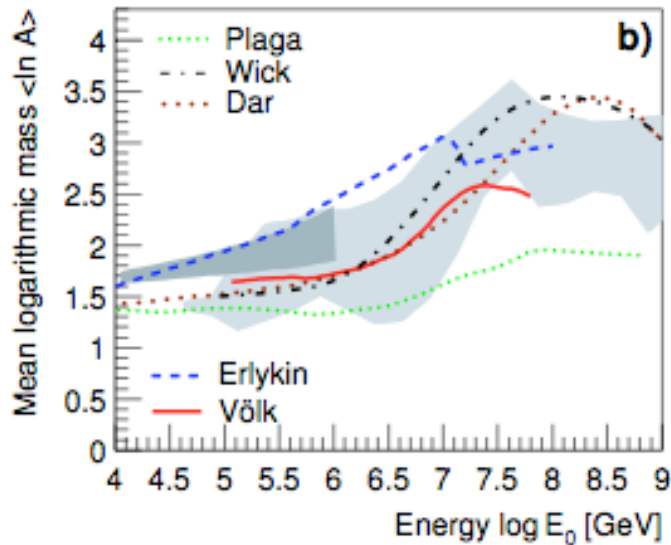
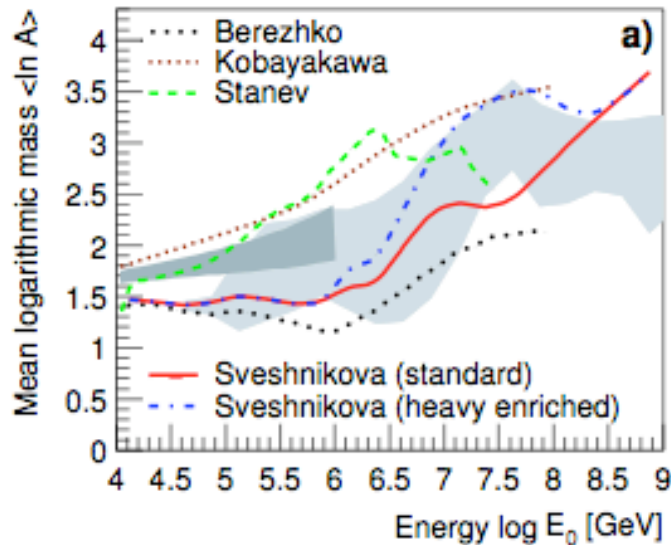
The Iron spectrum

The overlap direct/indirect is not reached
 but gap is smaller
 The best fit to Tracer+CRN globally gives
 $\gamma \sim 2.65$



acceleration in SNRs

Diffusion in the Galaxy



acceleration in GRBs

propagation in Galaxy

Direct measurements
 EAS measurements